


Research Article

PDGFR α -lineage origin directs monocytes to trafficking proficiency to support peripheral immunityYu-Tung Li¹ , Sho Yamazaki², Eiichi Takaki², Yuya Ouchi², Tomomi Kitayama² and Katsuto Tamai¹¹ Department of Stem Cell Therapy Science, Graduate School of Medicine, Osaka University, Suita, Japan² StemRIM Inc., Ibaraki, Osaka, Japan

Multiple embryonic precursors give rise to leukocytes in adults while the lineage-based functional impacts are underappreciated. Mesodermal precursors expressing PDGFR α appear transiently during E7.5–8.5 descend to a subset of Lin[−]Sca1⁺Kit⁺ hematopoietic progenitors found in adult BM. By analyzing a PDGFR α -lineage tracing mouse line, we here report that PDGFR α -lineage BM F4/80⁺SSC^{lo} monocytes/macrophages are solely Ly6C⁺LFA-1^{hi}Mac-1^{hi} monocytes enriched on the abluminal sinusoidal endothelium while Ly6C⁺LFA-1^{lo}Mac-1^{lo} macrophages are mostly from non-PDGFR α -lineage *in vivo*. Monocytes with stronger integrin profiles outcompete macrophages for adhesion on an endothelial monolayer or surfaces coated with ICAM-1-Fc or VCAM-1-Fc. Egress of PDGFR α -lineage-rich monocytes and subsequent differentiation to peripheral macrophages spatially segregates them from non-PDGFR α -lineage BM-resident macrophages and allows functional specialization since macrophages derived from these egressing monocytes differ in morphology, phenotype, and functionality from BM-resident macrophages in culture. Extravasation preference for blood PDGFR α -lineage monocytes varies by tissues and governs the local lineage composition of macrophages. More PDGFR α -lineage classical monocytes infiltrated into skin and colon but not into peritoneum. Accordingly, transcriptomic analytics indicated augmented inflammatory cascades in dermatitis skin of BM-chimeric mice harbouring only PDGFR α -lineage leukocytes. Thus, the PDGFR α -lineage origin biasedly generates monocytes predestined for BM exit to support peripheral immunity following extravasation and macrophage differentiation.

Keywords: Innate immunity · Integrins · Fate mapping · Cell trafficking · PDGFR α 

Additional supporting information may be found online in the Supporting Information section at the end of the article.

Introduction

Endothelium acts as the gate keeper to control leukocyte trafficking to and from circulation. A low level of trafficking is

allowed under homeostasis for leukocyte turnover and immune surveillance. This gateway widens in inflamed tissues as the local endothelium becomes activated and expresses surface molecules to facilitate leukocyte recruitment [1]. Capture of fast-flowing leukocytes in the circulation into rolling cells on endothelium requires interactions with endothelial selectins [2]. Together with chemokines and additional lectin interactions, leukocyte integrins are activated by inside-out signaling to increase adhesiveness

Correspondence: Yu-Tung Li and Katsuto Tamai
e-mail: tomli_yt@sts.med.osaka-u.ac.jp; tamai@gts.med.osaka-u.ac.jp

which eventually decelerates the rolling to full arrest on endothelial cell (EC) adhesion molecules (CAMs) [3–5]. Integrin signals then propagate to enable leukocyte crawling to an appropriate exit site for transendothelial diapedesis [6,7].

Monocyte is a cardinal component of the innate immunity derived from hematopoietic stem and progenitor cells (HSPC) via definitive hematopoiesis in BM. HSPC give rise to common myeloid progenitor which then sequentially produces macrophage and DC progenitor (MDP) and a monocyte/macrophage lineage-committed common monocyte progenitor (cMoP) [8,9]. The heterogeneous monocyte population contains Ly6C⁺ classical and Ly6C⁻ nonclassical cells. Ly6C⁻ monocytes in blood potentially originate from Ly6C⁺ cells [10–12]. Monocyte egress from BM into circulation requires transendothelial migration controlled by the CCL2-CCR2 chemotactic axis [13]. Although sinusoidal endothelium in BM is fenestrated, the fenestrae are impairment to cellular entities [14]. In addition, diapedesis across basement membrane might not be necessary as the basement membrane on the abluminal side of endothelium is discontinuous [15].

Upon inflammation, monocytes follow the typical extravasation cascade to assess inflamed tissues with an exception of certain nonclassical monocytes which constantly crawl on the luminal surface of the endothelium [16]. Extravasated monocytes could differentiate into DCs or macrophages and have extended impacts on inflammation. Contrasting the homeostatic nature of tissue-resident macrophages (trMF) in steady state, monocyte-derived macrophages are generally inflammatory. Since macrophage is phenotypically plastic and adapts to the surrounding microenvironment [17], trMF presumably support inflammation as well amidst the proinflammatory neighborhood. Rendezvoused pool of macrophages performs various functions including antigen presentation, cytokine production, clearance of pathogens, and apoptotic cells and efferocytosis [18].

The functional correlation of monocyte/macrophage ontology is unclear. trMF could originate from embryonic precursors or monocytes depending on the tissue. Alveolar macrophage, an embryonic-derived and self-sustained macrophage [19], when irradiated and replaced by BM-derived macrophages, adopted almost an identical enhancer profile as the native alveolar macrophages [17], suggesting the cellular plasticity might have overridden any ontology-driven difference. Unlike Flk⁺, mesodermal hemogenic endothelium, which essentially lineage to all hematopoietic cells in adults via a process called endothelial-to-hematopoietic transition [20], mesodermal precursors expressing PDGFR α (Pa) which temporarily emerge within a narrow window between E7.5 and E8.5 only give rise to a subset of hematopoietic cells [21]. In adults, Pa is considered as a marker for mesenchymal cells [22], a lineage distinct from either endothelial or hematopoietic cells. We, hence, hypothesize monocytes and macrophages derived from the Pa⁺ embryonic precursors might inherit lineage-based functionality difference from the rest.

Here, we have analyzed whether monocytes and macrophages derived from Pa⁺ precursors present functional difference in vivo from nonlineage counterparts. Using lineage tracing mice labeling progeny cells of PDGFR α -lineage with tdTomato, we

demonstrate that the PDGFR α -lineage cells in BM F4/80⁺SSC^{lo} monocytes/macrophages are mostly egressing Ly6C⁺ monocytes. These cells show stronger integrin expression and are more adhesive on endothelial CAMs than BM macrophages which are mostly non-PDGFR α -lineage. Egressing LFA-1^{hi}Mac-1^{hi} monocytes, enriched for PDGFR α -lineage cells, generate distinct macrophages from BM-resident macrophages. In addition, we profiled the extravasation preference of PDGFR α -lineage monocytes and found classical monocytes preferentially enter skin and colon and subsequently modify the resident pool of macrophages. Finally, with BM transplantation and transcriptomic analytics, we show that the extravasation ease of PDGFR α -lineage leukocytes aggravates the inflammatory responses in the dermal stroma during atopic dermatitis (AD).

Results

PDGFR α -lineage contributes to peripheral monocytes but little to BM-resident macrophages

We investigated the contribution of PDGFR α -lineage to HSPC and differentiated leukocytes in BMs using PDGFR α -lineage tracing mice, where *Pdgfra* promoter on a BAC clone drives the expression of Cre-recombinase that subsequently labels progeny cells with tdTomato. Lineage- Sca1⁺ Kit⁺ (LSK) cells contain HSC and multipotent progenitors, which give rise to LS-K and LSK- oligopotent or lineage-restricted progenitors. Observed in multiple bone types, these three upstream progenitor populations contain 27.6–33.8% cells of PDGFR α -lineage (Figure 1A-C and Supporting information Figure S1). Our measurements align with a previous study which pulse traced the descendant cells of PDGFR α -expressing precursors by tamoxifen-inducible Cre-recombinase at E8.0 and labeled 25% of LSK cells in fetal liver by E15.5.²¹ Nevertheless, the Pa(lin)⁺ fraction falls to an average of 13.4% ($\pm 0.4\%$) in F4/80⁺SSC^{lo} monocytes/macrophage compartment. Using EdU to pulse-label freshly synthesized cells from proliferating progenitors, we verified the PDGFR α -lineage contribution has been reduced since biogenesis of BM F4/80⁺SSC^{lo} monocytes/macrophage (Figure 1D). Within 4-h, there tends to be more PDGFR α -nonlineage F4/80⁺SSC^{lo} being labeled by EdU (+27.1% [$\pm 4.5\%$]) suggesting PDGFR α -lineage cells might be generated at a slower rate than nonlineage counterparts (Figure 1D). This decline in PDGFR α -lineage contribution could also be observed, but to, much milder extent, in BM CD115⁺ monocytes (21.8% ($\pm 1.2\%$)), neutrophils (24.2% ($\pm 1.4\%$)), and B cells (17.1–22.5% depending on the maturation stages) (Figure 1A-C and Supporting information Figure S2). Only slight declines in PDGFR α -lineage contribution were observed in downstream progenitors of monocytes and neutrophils, Kit+Ly6C+PECAM-1+ cMoP and the Kit+Ly6C+PECAM-1- neutrophil progenitors [23], which respectively harbor 25.7% ($\pm 1.1\%$) and 23.4% ($\pm 1.6\%$) cells from PDGFR α -lineage (Figure 1A-C and Supporting information Figure S1). These PDGFR α -lineage hematopoietic cells are solely descended from embryonic,

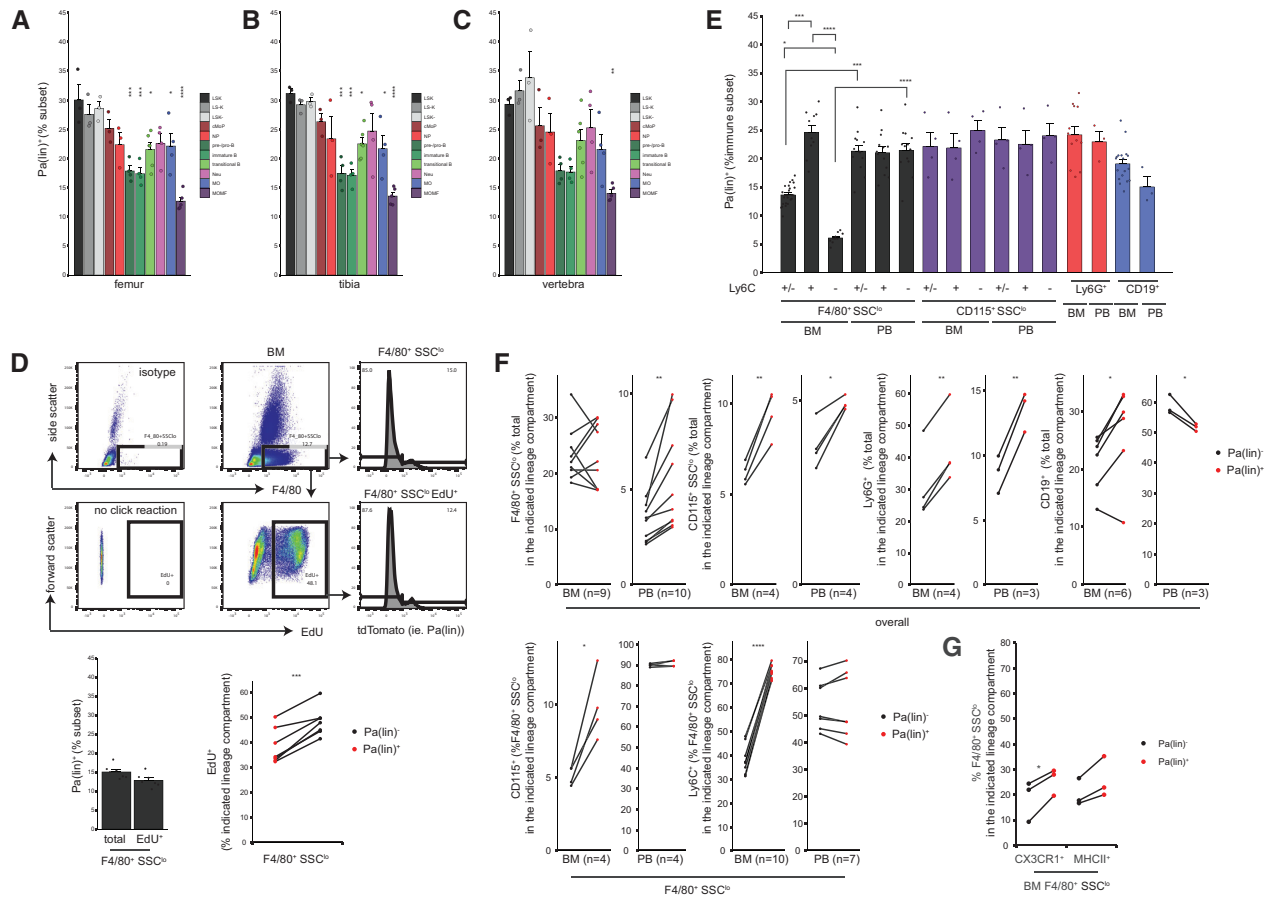


Figure 1. F4/80⁺SSC^{lo} BM monocytes/macrophages derived from PDGFR α ⁺ mesodermal origin contains a higher mobile fraction that egresses to blood in vivo. (A–C) Bone marrow (BM) cells of vertebra, femur, and tibia were isolated from PDGFR α -lineage tracing mice and the contribution of PDGFR α lineage was measured by flow cytometry. In BM, LSK progenitors, neutrophil progenitors, common monocyte progenitors (n = 3 mice each, 3 batches), CD19⁺ B cells (CD23[−]CD24[−]IgM[−] pre-/pro-B, CD23[−]CD24⁺IgM⁺ immature B and CD23⁺CD24⁺ transitional B, n = 4–6 mice, 3 batches), Ly6G⁺ neutrophils (n = 4 mice, 4 batches), CD115⁺SSC^{lo} monocytes (n = 4 mice, 1 batches), and F4/80⁺SSC^{lo} monocytes/macrophages (n = 5 mice, 3 batches) were analyzed. Samples in (A–C) were compared to LSK cells. (D) Four hours after intraperitoneal administration of 1 mg EdU, PDGFR α -lineage contribution in freshly generated EdU⁺ BM monocytes/macrophages and EdU-labelling efficiency in Pa(lin)^{+/−} F4/80⁺SSC^{lo} were measured (n = 7 mice, 2 batches). (E) PDGFR α -lineage contribution in F4/80⁺SSC^{lo} Ly6C^{+/−} PB monocytes (n = 13 mice, 6 batches), CD115⁺SSC^{lo} Ly6C^{+/−} PB monocytes (n = 4 mice each, 1 batch), neutrophils and B cells (n = 3 mice each, 1 batch each) were compared to BM counterparts average of all bone types measured in (A–C). (F) Leukocyte subset composition in Pa(lin)⁺ and Pa(lin)[−] compartments of total cells (upper) or F4/80⁺SSC^{lo} cells (lower) in BM and PB were compared within individual mice (n numbers indicated in brackets). (G) Proportion of CX₃CR1⁺ (n = 3 mice, 1 batch) or MHCII⁺ (n = 3 mice, 2 batches) cells in Pa(lin)⁺ and Pa(lin)[−] F4/80⁺SSC^{lo} monocytes/macrophages were quantified within individual mice. Error bars, SEM. Individual data are represented by dots. For all measurement, one mouse per experiment. Groups were compared by one-way ANOVA followed by Tukey's multiple comparisons in (A–C and E), two-sample t-test in (D) comparing Pa(lin)⁺ proportion and paired t-test in (D) comparing EdU labeling between Pa(lin)^{+/−} within individual mice and in (F–G). *p < 0.05, **p < 0.01, ***p < 0.001, ****p < 0.0001.

but not from adults, PDGFR α ⁺ precursors, as we detected are <1% PDGFR α -expressing cells among LSK, myeloid progenitors, F4/80⁺, Ly6G⁺, or CD19⁺ compartments in adult BM using a knock-in reporter mouse line [22], where H2B-GFP expression is driven by endogenous *Pdgfra* promoter in one allele (Supporting information Figure S3).

Since F4/80⁺SSC^{lo} BM cells contain a mixed population of monocytes and macrophages, we examined the CD115⁺ monocyte content within this population and the expression of F4/80 among the whole CD115⁺ monocyte population. In BM, F4/80⁺SSC^{lo} BM cells contains only 5.8% (\pm 0.4%) CD115⁺ monocytes. Nevertheless, these F4/80⁺CD115⁺ monocytes are the major trafficking fraction as F4/80⁺SSC^{lo} cells in peripheral

blood (PB) contains 90.1% (\pm 0.4%) CD115⁺ cells. F4/80 expression marks 29.3% (\pm 1.9%) of BM CD115⁺ monocytes with 25.3% (\pm 1.7%) and 72.3% (\pm 1.1%) of Ly6C⁺ classical and Ly6C[−] non-classical monocytes (cMO and ncMO), respectively, being labeled. In PB, intermediate F4/80 expression could be detected on both cMO and ncMO (Supporting information Figures S4 and S5). Hence, BM F4/80⁺SSC^{lo} cells contain macrophages and a subset of CD115⁺ monocytes.

Within the BM F4/80⁺SSC^{lo} monocytes/macrophages population, we found that the PDGFR α -lineage contribution deficiency is specific to the Ly6C[−] compartment. The fact that F4/80⁺Ly6C[−] cells receive a significantly lower PDGFR α -lineage contribution than CD115⁺Ly6C^{+/−} monocytes indicates macrophages in BM

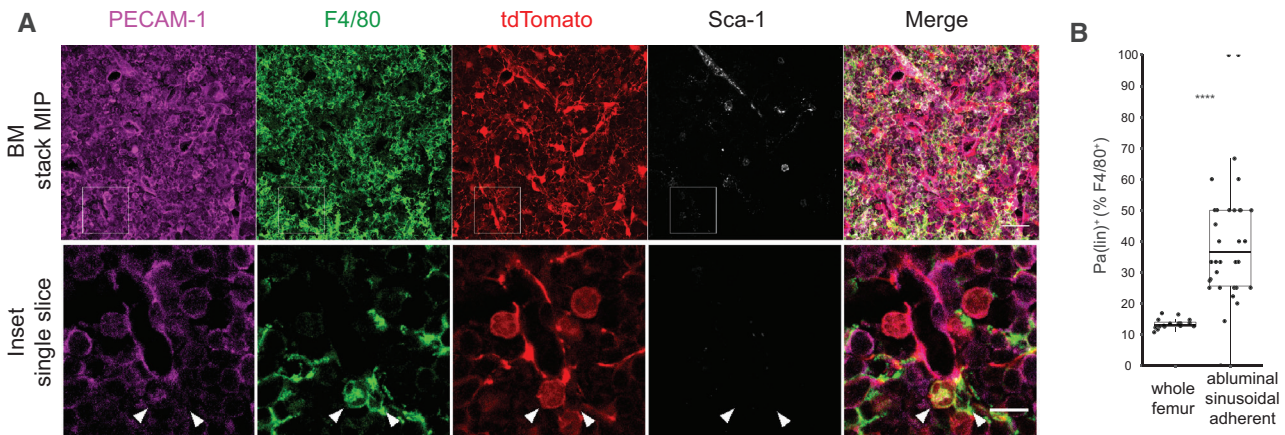


Figure 2. The abluminal surface of sinusoidal endothelium are enriched for PDGFR α -lineage F4/80 $^{+}$ cells. (A) Spatial correlation between PDGFR α -lineage monocytes and sinusoidal abluminal surface was examined in 60 μ m-thick BM cryosection by three-dimensional confocal microscopy. A representative image of five experiments (upper panel) is shown as maximal intensity projection (MIP). Scale, 30 μ m. Inset was shown as a single slice (lower panel). Left arrow indicates a Pa(lin) $^{+}$ monocyte and right arrow indicates a Pa(lin) $^{-}$ monocytes. Scale, 10 μ m. (B) Proportion of Pa(lin) $^{+}$ monocytes on sinusoids ($n = 177$ monocytes on 34 sinusoids pooled from five mice) was quantified and compared to the global proportion of Pa(lin) $^{+}$ monocytes in femur BM ($n = 16$ mice, 6 batches) measured by flow cytometry. Error bars, SEM. Individual data are represented by dots. One mouse per experiment. Images are representative of five independent experiments. Groups were compared by Mann–Whitney U-test. **** $p < 0.0001$.

being mostly derived from non-PDGFR α -lineage monocytes (Figure 1E). On the other hand, both PDGFR α -lineage and nonlineage contribute to BM F4/80+Ly6C $^{+}$ cells at a similar ratio to CD115+Ly6C $^{+}$ monocytes (Figure 1E). Previous BrdU pulse-trace experiments have shown CCR2+Ly6C $^{+}$ cMO as the monocyte subset that readily egresses to circulation [10,11] and gives rise to blood Ly6C $^{-}$ ncMO in situ [10]. Egress efficiency of these cMO, either F4/80 $^{+}$ or CD115 $^{+}$, are equivalent between PDGFR α -lineage/nonlineage as the Pa(lin) $^{+}$ fraction do not differ between BM and PB. Similarly, egress efficiency of Ly6G $^{+}$ neutrophils and CD19 $^{+}$ B cells do not differ by PDGFR α -lineage (Figure 1E). In general, PDGFR α -lineage BM cells contain more CD115 $^{+}$ monocytes and Ly6G $^{+}$ neutrophils (Figure 1F, upper panel). Among BM F4/80+SSC lo monocytes/macrophages, PDGFR α -lineage is enriched for egressing CD115 $^{+}$ and Ly6C $^{+}$ cells (Figure 1F, lower panel and Supporting information Figures S4 and S5) but not for CX3CR1 $^{+}$ or MHCII $^{+}$ cells (Figure 1G). Taken together, while the non-PDGFR α -lineage F4/80+SSC lo encompasses both egressing monocytes and BM-resident monocytes that differentiate to macrophages, the PDGFR α -lineage mostly generates Ly6C $^{+}$ egressing monocytes.

PDGFR α -lineage F4/80 $^{+}$ monocytes are enriched on the abluminal surface of femoral endothelium

Sca-1 $^{-}$ PECAM-1 $^{+}$ sinusoids have been reported as major trafficking sites [24]. If PDGFR α -lineage cells are restricted to the trafficking monocytes, we hypothesize these cells might populate the surface of these trafficking portals. Three-dimensional confocal examination of adherent F4/80 $^{+}$ cells (in directly contact) on the sinusoidal abluminal surface revealed 36.7% ($\pm 3.6\%$) of the cells observed were from PDGFR α -lineage, a significantly

higher proportion than the global Pa(lin) $^{+}$ fraction of F4/80 $^{+}$ monocytes/macrophages in the whole femur as measured by flow cytometer (Figure 2A and B). Enriched Pa(lin) $^{+}$ F4/80 $^{+}$ cells on the abluminal endothelium suggest BM monocytes, but not macrophages, are in close association with these sinusoidal trafficking portals.

Integrins favor monocyte over macrophage adhesion on ECs or CAMs in vitro

We tested whether PDGFR α -lineage-rich monocyte fraction of F4/80 $^{+}$ SSC lo preferentially adheres on ECs, a necessary step in transendothelial migration. Bone marrow cells (BMC) obtained from the PDGFR α -lineage tracing mice were allowed to adhere on resting or TNF- α stimulated primary EC isolated from WT skin in Mg $^{2+}$ and Ca $^{2+}$ containing serum-free medium. After dissociating adherent cells from the endothelial monolayer, the Pa(lin) $^{+}$ fraction among adherent F4/80 $^{+}$ SSC lo was measured and compared to the input. Since Pa(lin) $^{+}$ cells in F4/80 $^{+}$ SSC lo are restricted to monocytes (Figure 1E), an increased Pa(lin) $^{+}$ fraction after adhesion indicates monocytes better compete over Pa(lin) $^{-}$ -rich macrophages for the adherent surface. After adhesion on resting EC, we recorded a significant increase in the Pa(lin) $^{+}$ fraction of F4/80 $^{+}$ SSC lo , ranging from +50.3% ($\pm 7.2\%$) to +80.0% ($\pm 2.6\%$). TNF- α -stimulated EC supported at least five-fold more adhesion than at rest and similarly, stronger adhesion for PDGFR α -lineage-rich F4/80 $^{+}$ SSC lo monocytes was observed with similar magnitude ranges from +41.7% ($\pm 3.7\%$) to +71.2% ($\pm 3.0\%$) (Figure 3A and B).

Since adhesion on EC is solely supported by interaction with CAMs, we assessed if ICAM-1 or VCAM-1 alone, the two major endothelial CAMs, suffices to favor adhesion for

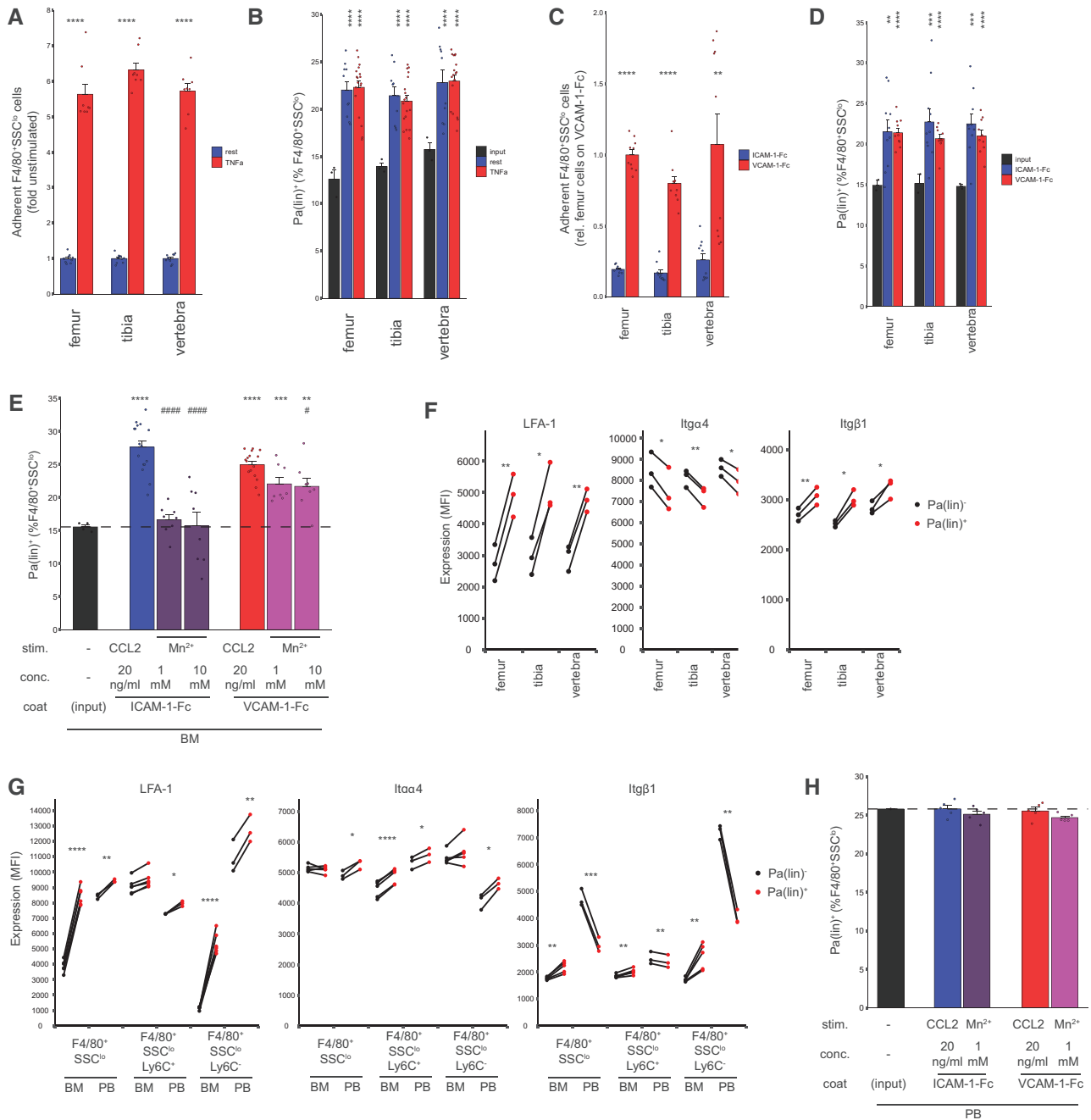


Figure 3. Altered integrin expression and activation support better adhesion of PDGFR α -lineage F4/80⁺SSC^{lo} on endothelial cell adhesion molecules. (A–B) Bone marrow cells containing both PDGFR α -lineage and nonlineage BM cells were allowed to competitively adhere on resting (blue) or TNF- α inflamed (red) primary dermal endothelial cells. (A) Adherent F4/80⁺SSC^{lo} cells were dislodged and enumerated. (B) Proportion of PDGFR α lineage in adherent F4/80⁺SSC^{lo} were compared to that in input cells (black). A total of $n = 10$ each from two independent experiments for resting conditions and $n = 18$ each from three independent experiments for TNF- α stimulation. (C–D) The competitive adhesion assay described in (A–B) was repeated on surfaces coated with ICAM-1-Fc (blue) or VCAM-1-Fc (red). $n = 10$ each from two independent experiments. Adherent cells were quantified in (C) and the proportion of Pa(lin)⁺ F4/80⁺SSC^{lo} in adherent cells were compared to input in (D). (E) Experiment described in (C–D) was repeated using either CCL2 or MnCl₂ ($n = 16$ and 8 pooled from two independent experiments) as the stimulus. (F–G) Expression of LFA-1, integrin $\alpha 4$ and integrin $\beta 1$ on surfaces of Pa(lin)⁺ and Pa(lin)⁻ F4/80⁺SSC^{lo} from indicated tissues and subsets were measured by flow cytometry. $n = 3$ mice in three batches for (F), $n = 3$ mice in one batch for PB in (G) and $n = 5$ –6 mice in two batches for BM in (G), one mouse per experiment. (H) Experiment described in (E) was repeated with PB cells ($n = 5$ each in an experiment with cells pooled from four mice). Error bars, SEM. Individual data are represented by dots. Groups were compared by two-sample t-test in (A and C), one-sample t-test against input in (B and D) and paired t-test in (F–G). In (E), groups were compared against the CCL2 stimulation ctrls by one-way ANOVA followed by Tukey's multiple comparisons and by one-sample t-test against input. # $p < 0.05$, #### $p < 0.0001$ against CCL2 stimulation. * $p < 0.05$, ** $p < 0.01$, *** $p < 0.001$, **** $p < 0.0001$.

PDGFR α -lineage-rich monocytes. The competitive adhesion assay was repeated on a surface immobilized with purified proteins of either ICAM-1-Fc or VCAM-1-Fc in the presence of CCL2 as the stimulating chemokine. Similar to the endothelial surface, adhesion on both immobilized ICAM-1-Fc and VCAM-1-Fc led to monocyte enrichment in magnitudes comparable to that on EC (Figure 3C and D). Leukocytes interact with endothelial CAMs via integrins which need to be activated into a high affinity and open conformation for ligand interaction. To delineate whether the better adhesion support for PDGFR α -lineage-rich monocytes is due to more efficient activation, in the competitive adhesion assay, we replaced the stimulating reagent of CCL2 with Mn2+, which bypasses the inside-out signaling and forces integrins into high-affinity open conformation [25,26]. Mn2+ stimulation reduced the adhesion advantage of Pa(lin)+-rich monocytes fully on ICAM-1-Fc and partially on VCAM-1-Fc (Figure 3E). The partial reduction of the adhesion advantage after bypassing the inside-out signal suggests integrin heterodimer expression, besides activation, also contributes to the adhesion advantage of marrow monocytes over macrophages on endothelial CAMs.

LFA-1 (Itg α L/ β 2) and VLA-4 (Itg α 4/ β 1) are the major integrins utilized by leukocytes to interact with ICAM-1 and VCAM-1, respectively [27]. To directly examine if integrin expression differs between PDGFR α -lineage and between monocytes and macrophages, we measured the expression of LFA-1, Itg α 4, and Itg β 1 on the surface of marrow F4/80+SSC^{lo} monocytes/macrophages. While Pa(lin)+ monocytes express significantly more LFA-1 than Pa(lin)- monocytes/macrophages, individual expression of Itg α 4 and Itg β 1 do not massively differ (Figure 3F). Stronger LFA-1 expression was also detected on F4/80+SSC^{lo}Ly6C+ monocytes than on Ly6C- macrophages (Figure 3G). After entry to circulation, monocytes express high levels of integrin which do not differ much by PDGFR α -lineage (Figure 3G). Accordingly, PB Pa(lin)+ monocytes do not preferentially adhere on the CAMs upon chemokine or Mn2+ stimulation (Figure 3H).

BM monocytes generate macrophages functionally distinct from marrow-resident macrophages

When the expression of Itg α M, the integrin alpha chain of another ICAM-1-binding integrin Mac-1, on BM F4/80+SSC^{lo} monocyte/macrophage was measured, we detected a high expression of Itg α M on PDGFR α -lineage F4/80+SSC^{lo} monocytes. Indeed, Pa(lin)+ BM F4/80+SSC^{lo} monocytes are essentially LFA-1^{hi} Itg α M^{hi} whereas Pa(lin)- BM F4/80+SSC^{lo}, comprising of monocytes and macrophages, contain both LFA-1^{hi} Itg α M^{hi} and LFA-1^{lo} Itg α M^{lo} cells (Figure 4A). Expression levels of LFA-1 and Itg α M are similar between PDGFR α -lineage/nonlineage LFA-1^{hi} Itg α M^{hi} monocytes (only differing by 5.0 \pm 1.0% and 6.3 \pm 1.5% for LFA-1 and Itg α M, respectively). PDGFR α -lineage contribution in LFA-1^{hi} and/or Itg α M^{hi} F4/80+SSC^{lo} are similar to that in F4/80+ or CD115+ Ly6C+ cMO in BM and PB, confirming this population contains mostly monocytes (Figures 1E and 4B). In a pulse-

trace experiment by EdU to follow the kinetics of freshly generated LFA-1^{hi} Itg α M^{hi} and LFA-1^{lo} Itg α M^{lo} F4/80+SSC^{lo} (M^{hi2} and M^{lo2}), we found that at 4 h post- EdU administration, EdU+ cells could be detected among both M^{hi2} and M^{lo2} with the labeling in M^{lo2} overwhelming. Frequency of EdU+ M^{lo2} declined after 1 day accompanying increased frequency of EdU+ M^{hi2} (Figure 4C). This temporal sequence of EdU labeling suggests M^{lo2} might contains some monocytes, mostly from non-PDGFR α -lineage, that have turned LFA-1^{hi} Itg α M^{hi}. Direct EdU tracing of non-PDGFR α -lineage F4/80+SSC^{lo} cells confirmed this conversion (Supporting information Figure S6).

Macrophages derived in vitro from M^{hi2} and M^{lo2} (Mac^{hi2} and Mac^{lo2}), respectively, corresponding to peripheral macrophages differentiated from trafficking monocytes and BM-resident macrophages, expressed similar amount of Itg α M. CD64 expression was higher on Mac^{hi2} (Figure 4D). Mac^{lo2} tended to be more roundish whereas Mac^{hi2} were more elongated and spikier (Figure 4E). Macrophage differentiation efficiency is unaffected by lineage origin as Pa(lin)+ proportion in F4/80+ cells remained unaltered after differentiation (Supporting information Figure S7). We explored by bulk RNA sequencing whether Mac^{hi2} and Mac^{lo2} might perform different functions. In these macrophages, expression of 3949 genes significantly differed by the originating F4/80+SSC^{lo}. Functional enrichment analyses of these genes indicated Mac^{hi2} differs from Mac^{lo2} by stronger expression of cell cycle regulating genes whereas gene expression in Mac^{lo2} tilts toward immune responses (Figure 4F). Mac^{hi2} is characterized by high transcription factor (TF) activities of cell cycle relevant TF such as E2F family, forkhead box protein M1 and Myc. In contrast, higher TF activities relevant to cell activation, such as STAT1/3, PU1, and NF-kB, were detected in Mac^{lo2} (Figure 4G). Transcript expression of common macrophage markers did not differ between Mac^{hi2} and Mac^{lo2}. Interestingly, Mac^{hi2} expresses high levels of *Siglec-1* and *Cx3cr1*, both of which are known markers of marrow-resident macrophages, suggesting a portion of M^{hi2} has remained in BM and given rise to Mac^{hi2}. In contrast, Mac^{lo2} expresses low transcript levels of *Siglec-1* and *Cx3cr1* but high levels of *Cxcr4* and potentially represent another macrophage subset in BM (Figure 4H). In vivo, a limited fraction of F4/80+Ly6C-CD64+Siglec-1+ BM macrophages express CXCR4 while most F4/80+Ly6C-CD64+Siglec-1- cells are CXCR4+ (Figure 4I). When we re-examined our previous single-cell RNA sequencing datasets (GSE159535) and mapped PB monocytes to BM monocytes/macrophages, PB monocytes overlay with cluster 3 and 1 of BM monocytes/macrophages, demonstrating cluster 3 and 1, but not cluster 2, of BM monocytes/macrophages are sources of egressed monocytes (Supporting information Figure S8A). Meanwhile, Siglec-1+ macrophages were exclusively found in cluster 1 and, thus, are likely derived from egress-ready M^{hi2}-like monocytes. Stronger *Cxcr4* signal was detected in cluster 2 and these macrophages are derived from BM-resident M^{lo2}-like monocytes (Supporting information Figure S8B). Accordingly, Mac^{hi2}-like F4/80+Ly6C-CD64+Siglec-1+CXCR4- has more PDGFR α -lineage descendants than Mac^{lo2}-like F4/80+Ly6C-CD64+Siglec-1-CXCR4+ macrophages

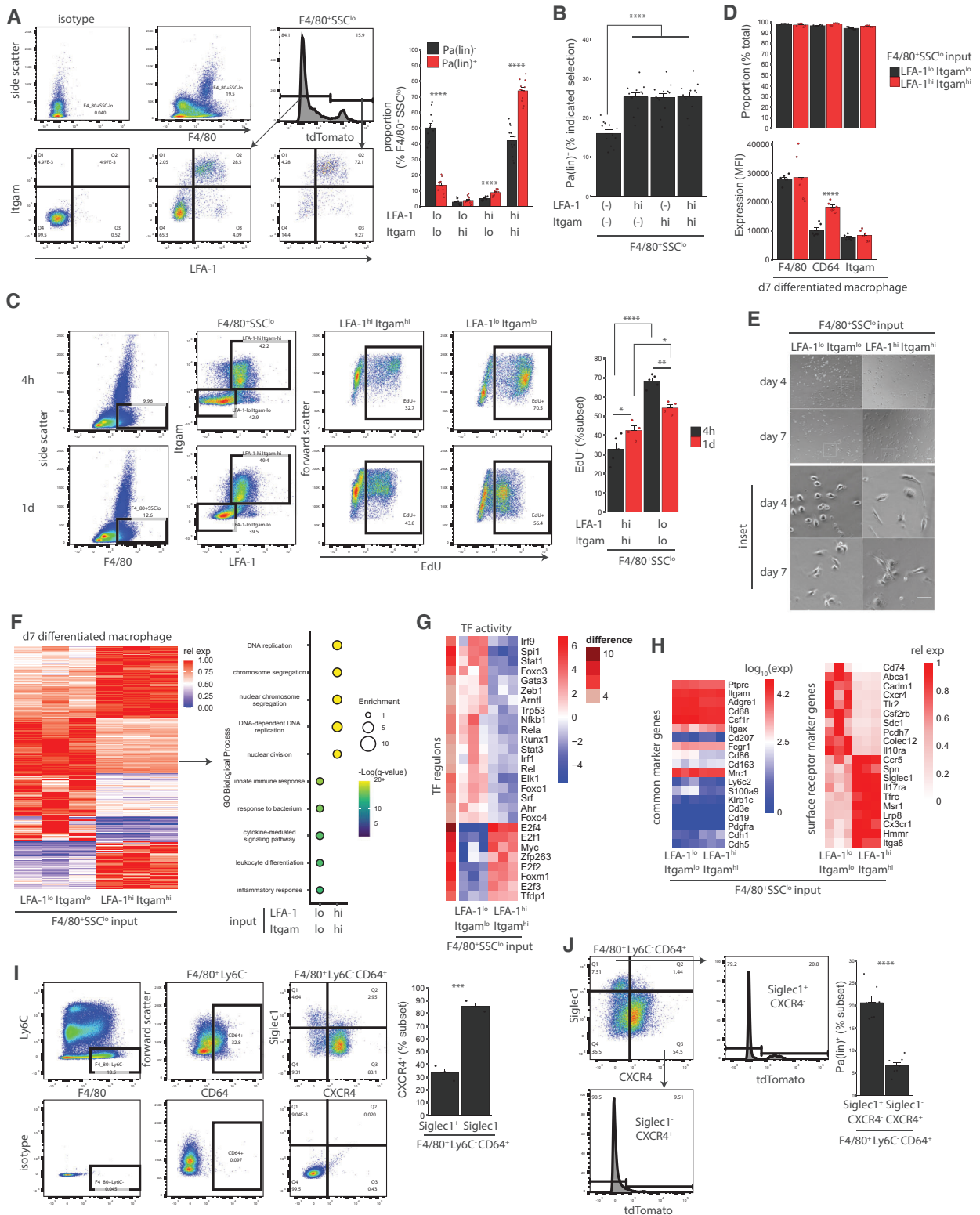


Figure 4. Distinct expression of LFA-1 and Mac-1 support egress of PDGFR α -lineage F4/80⁺SSC^{lo} and determine the functional profiles of differentiated macrophages. (A) BM cells were isolated from PDGFR α -lineage tracing mice and measured for expression of LFA-1 and Itg α_M . (B) Fraction of Pa(lin)⁺ cells was measured in all F4/80⁺SSC^{lo} cells, in the LFA-1^{hi}, Itg α_M ^{hi}, or LFA-1^{hi} Itg α_M ^{hi} fractions. n = 12 mice, four batches. (C) Four hours or 10 day (n = 5 or 4 mice pooled from two batches) after intraperitoneal administration of 1 mg EdU to WT mice, frequencies of EdU⁺ BM monocytes in the indicated subsets were measured. (D) LFA-1^{hi} Itg α_M ^{hi} and LFA-1^{lo} Itg α_M ^{lo} F4/80⁺SSC^{lo} monocytes were isolated from WT and differentiated in M-CSF containing medium for 7 days. Expression of indicated macrophage markers were measured by flow cytometry. n = 6 differentiation from three mice (two differentiation per experiment, three experiments). (E) Morphology of the derived macrophages shown. Scale, 100 μ m (upper) and 50 μ m

(Figure 4J). Overall, we show the Pa(lin)⁺-rich BM egressing monocytes differentiate to macrophages that differ in functionality from Pa(lin)⁻ BM-resident macrophages.

Extravasation preference for PDGFR α -lineage monocytes is controlled by tissue-specific determinants

We next asked if extravasation of monocytes differs by PDGFR α -lineage origin. We have here examined *in vivo* the competitive extravasation of PDGFR α -lineage/nonlineage monocyte to tissues (skin, peritoneum, and colon) under steady state and inflammation.

Local acute inflammation was induced intradermally by injecting 1 μ g LPS or saline ctrl to different dorsal areas of the same mouse. Skin samples were collected overnight and analyzed by flow cytometry. Comparing the two injection areas verified a LPS-specific inflammation with a 5.6-fold (\pm 2.1-fold) rise in the infiltrated F4/80⁺ MHCII⁻ Ly6C⁺ cMO in the F4/80⁺ compartment (Figure 5A). To determine if extravasation efficiency of monocytes differs by PDGFR α -lineage origin, we compared the Pa(lin)⁺ fractions in pre-extravasated monocytes in the circulation and postextravasated monocytes in LPS-stimulated skin. To our surprise, in contrast to 21.6% (\pm 2.1%) of Pa(lin)⁺ monocytes in the blood, the Pa(lin)⁺ fraction expanded by 57% after extravasation to the inflamed skin (Figure 5B). Interestingly, this effect was specifically observed with cMO (Figure 5B and C).

To trigger chronic inflammation in the AD model, we applied 5 nmol MC903 which stimulates production of TSLP from keratinocytes [28] on dorsal skin bidaily or tridaily for six times. Thickened and/or reddened inflamed area was monitored in time course. The MC903 treatment induced a progressive inflammation that peaked on day 11 (Figure 5D). Monocyte influx into the inflamed skin was verified (Figure 5E) and extravasation efficiency of PDGFR α -lineage monocytes was examined on day 14. Similar to LPS stimulation, enhanced extravasation was observed with PDGFR α -lineage cMO. Pa(lin)⁺ cells constituted 24.1% (\pm 1.2%) of the pre-extravasated PB monocytes and 37.6% (\pm 3.6%) in the postextravasated population in the skin (Figure 5F and Supporting information Figure S9). Extravasation of ncMO was unaffected (Figure 5G). In addition, no specific expansion of PDGFR α -lineage monocytes in BM was evident (Supporting information Figure S10). We found that F4/80⁺ MHCII⁺ dermal macrophages in both healthy and AD skin receive major PDGFR α -lineage contribution (Figure 5H and Supporting infor-

mation Figure S11). Using 3D-confocal microscopy to locate large and irregular-shaped macrophages in AD skin, we observed an agreeing proportion of 38% of macrophages being from PDGFR α -lineage (Supporting information Figure S12). Since dermal macrophages are continuously replenished by extravasated monocytes even under homeostasis [29], it suggests that the selective extravasation of PDGFR α -lineage cMO has shaped the lineage composition in dermal macrophages. When the AD macrophage composition was analyzed by single-cell RNA-sequencing, three transcriptomic subtypes differing in surface markers, cytokine expression, and transcription activities, were identified. PDGFR α -lineage macrophages manifested a higher ratio of subtype 1/2 than nonlineage (3.7 vs 1.4) (Supporting information Figure S13), implying the lineage origin could have altered the functional profile of the descendant macrophages.

The extravasation support to PDGFR α -lineage cMO and the subsequent macrophage formulating capability seems to be tissue-specific. In unstimulated peritoneal cavity (PC), there is a major F4/80^{hi} Ly6C⁻, a minor F4/80⁺ Ly6C⁻ macrophage populations, and \sim 5% F4/80⁺ Ly6C⁺ infiltrating cMO. TNF- α stimulation specifically expanded the relative proportion of Ly6C⁺ infiltrating cMO (Figure 5I and J and Supporting information Figure S14). PDGFR α -lineage contribution in F4/80^{hi} macrophages was slightly lower than that in infiltrating cMO, while equivalent PDGFR α -lineage contribution was observed in F4/80⁺ macrophages and cMO, suggesting F4/80⁺ macrophages being derived from infiltrating monocytes. Infiltrating cMO specifically contributing to F4/80⁺ macrophages has been described with LPS or thioglycolate stimulation [30]. Nevertheless, PDGFR α -lineage contribution in neither of these monocyte/macrophage compartments exceeded the level in blood, indicating PDGFR α -lineage monocytes had not been favored for peritoneal extravasation (Figure 5K). We further examined whether preferential extravasation of PDGFR α -lineage cMO could be observed in colon, yet another tissue receiving constant monocyte input [31]. Ly6C⁺ cMO constitutes 8.2% (\pm 1.2%) of F4/80⁺SSC^{lo} cells in colon lamina propria under steady state. PDGFR α -lineage contribution in these extravasated cMO (51.0% (\pm 3.3%)) significantly exceeded that in blood, thus, indicating supported extravasation of PDGFR α -lineage cMO. Similar enhancement could be observed in F4/80⁺MHCII⁺ macrophages (33.6% (\pm 1.1%)) (Figure 5L and Supporting information Figure S14) or F4/80⁺MHCII⁺CX3CR1⁺ macrophages (33.9% (\pm 1.8%)) (Supporting information Figure 15). Of note, PDGFR α -lineage contribution to macrophages in all these peripheral tissues are prominently higher than that in BM (Figure 4J), highlighting the roles of PDGFR α -lineage monocytes

(inset). Images are representative of four experiments. (F–H) Macrophages were derived from LFA-1^{hi} Itg α_M ^{hi} and LFA-1^{hi} Itg α_M ^{hi} F4/80⁺SSC^{lo} monocytes *in vitro* and analyzed by bulk RNA sequencing. (F) Significant differentially expressed genes were analyzed for functional enrichment (Gene Ontology Biological Process). Top five enriched functions are shown for each macrophages. (G) Transcription factor (TF) activities were measured for each macrophages. TF activities with >2 SD difference are shown. (H) Common markers and surface receptor markers distinguishing Mac^{hi2} and Mac^{lo2} are shown. n = 2 differentiation pooled per mouse, three mice in total for bulk RNA-seq. (I) F4/80⁺Ly6C⁻CD64⁺ WT BM macrophages were examined for expression distribution of Siglec-1 and CXCR4. n = 3 mice, one batch. (J) PDGFR α -lineage contribution to Siglec-1⁺CXCR4⁻ and Siglec-1⁻CXCR4⁺ cells among F4/80⁺Ly6C⁻CD64⁺ BM macrophages isolated from lineage tracing mice were measured. n = 7 mice, four batches. Error bars, SEM. Individual data are represented by dots. For (A–C) and (I–J), one mouse per experiment. Groups were compared by two-sample t-test in (A, D and I–J) and one-way ANOVA followed by Tukey's multiple comparisons in (B–C). *p < 0.05, **p < 0.01, ***p < 0.001, ****p < 0.0001.

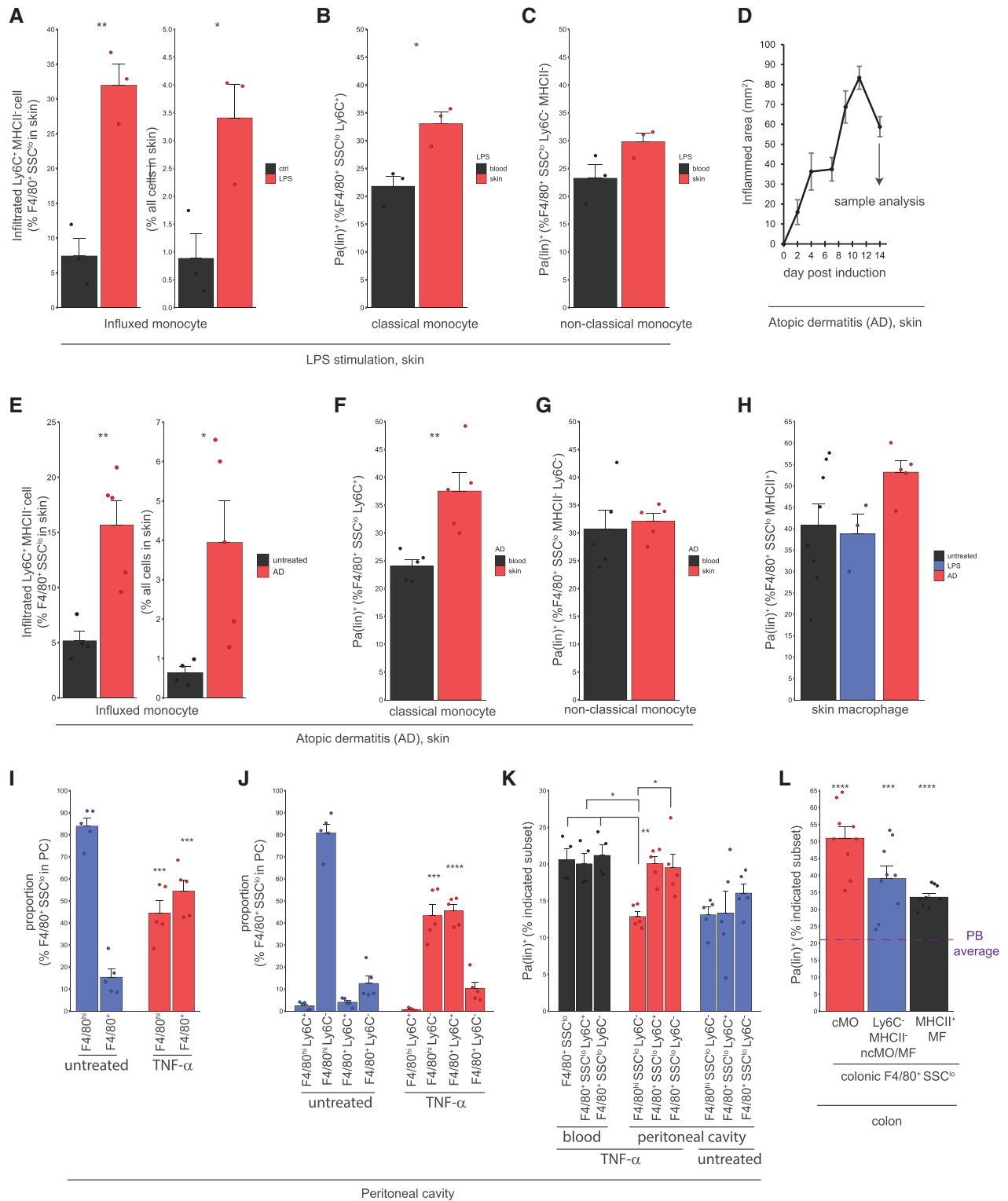


Figure 5. Recruitment preference for PDGFR α -lineage monocytes influences the lineage composition of tissue macrophages and is dictated by tissue-specific determinants under steady state and inflammation. (A–C) Mice received a single dose of LPS and saline ctrl on distinct dorsal skin areas. After overnight, skin was excised and analyzed for monocyte infiltration by flow cytometry. (A) Monocyte infiltration to LPS-stimulated area and ctrl area relative to F4/80⁺ cells (left) or all cells (right) were measured. Proportion of Pa(lin)⁺ classical monocytes (B) and nonclassical monocytes (C) in peripheral blood and inflamed skin are shown. (D) Six bi-/tridaily doses of MC903 were applied on dorsal skin and inflammation was monitored across 14-day time course. n = 10 mice, three induction batches. Inflamed skin was excised and analyzed on day 14 by flow cytometry. (E) Monocyte infiltration was analyzed (n = 4 [healthy, 2 batches] or 5 [AD, 2 induction batches]). Proportion of Pa(lin)⁺ classical monocytes (F) and nonclassical monocytes (G) were compared between peripheral blood and inflamed skin. n = 5

in peripheral defense. Hence, among the three examined tissues where at least a subset of macrophages receives turnover from infiltrating monocytes, we observed favored extravasation of PDGFR α -lineage cMO in skin and colon but not in peritoneum. These extravasated monocytes subsequently modulate the lineage composition of tissue macrophages.

Extravasated PDGFR α -lineage leukocytes differentially regulate the dermal environment

Since the extravasated pool of monocytes contained mixed PDGFR α -lineage origins, it renders investigation of the impacts of postextravasated PDGFR α -lineage monocytes to the tissue stromal environment difficult. To this end, we performed BM transplantation (BMT) to reconstitute the hematopoietic system of irradiated EGFP-Tg recipients with either Pa(lin)⁺ or Pa(lin)⁻ Lineage⁻ progenitors so that subsequent extravasation would be limited to a single PDGFR α -lineage origin. After 6-week recovery, PB was examined and verified approximately 90% blood cells being donor derived (Figure 6A). To assess in AD how the dermal environment might be influenced by the extravasated leukocytes, which were of single PDGFR α -lineage origin in these chimera mice, the mice were subjected to AD induction by MC903. Mice that had received Pa(lin)⁺ transplant presented more severe skin inflammation (1.98-fold on average weighed by inflammation severity) (Figure 6B). On day 14, skin was sampled for bulk RNA-sequencing and flow cytometric analysis of recruited leukocytes. Despite a lack of competitive control, the numbers of both recruited donor-derived CD45⁺ leukocytes and CD45⁺ F4/80⁺ monocytes/macrophages normalized to recipient-derived stromal cells tended to be higher in mice receiving Pa(lin)⁺ transplant (Figure 6C). In the sequencing analysis, 237 genes among the top half of expressed genes showed more than twofold expression difference between Pa(lin)⁺ and Pa(lin)⁻ BMT (Figure 6D). Gene ontology (GO) analysis of these genes indicated enriched inflammatory functions accompanying reduced dermal homeostatic functions with Pa(lin)⁺ BMT (Figure 6E). These results correlate well with the extravasation proficiency of PDGFR α -lineage monocytes. We sought to understand whether these affected processes by Pa(lin)⁺ BMT might associate with leukocyte PDGFR α -lineage origin independently of the extravasation effect. Leukocyte recruitment varied among the sequenced skin samples and fell into two sample clusters. All except one Pa(lin)⁻ BMT samples were found in the weak recruitment cluster whereas Pa(lin)⁺

BMT samples were divided (Figure 6F). Linear regressions were performed to investigate the independent contribution of extravasation and PDGFR α -lineage origin of the transplant to the top 10 enriched or depleted GO biological processes (GOBP) (see Materials and Methods for details). GOBP affected by Pa(lin)⁺ BMT are solely associated with extravasation (alone or interaction with BMT PDGFR α -lineage origin) but not to leukocyte PDGFR α -lineage origin alone (Figure 6G and Supporting information Table S1 and S2). Thus, the impacts to the dermal stromal environment brought about by PDGFR α -lineage leukocytes are large via extravasation. In addition, GSEA analysis [32], which relies on ranked expression fold ratio and avoid manual thresholding, reported consistent results with GO analyses and additionally indicated matrix metalloproteinases activation and ECM remodeling in Pa(lin)⁺ BMT (Supporting information Table S3).

Discussion

Leukocytes in adult mice lineage are from a cocktail of embryonic precursors [33]. Among these precursors are mesodermal embryonic progenitors, transiently expressing PDGFR α between E7.5 and E8.5, which give rise to PDGFR α -lineage leukocytes [21]. While previous simple transcriptomic comparison of PDGFR α -lineage/nonlineage CD45⁺ leukocytes found overall similarity [34], it had not assessed functional aspects, in particular, those swift responses solely regulated by post-transcriptional mechanisms, of specific immune compartments. Here, by following the trafficking dynamics of F4/80⁺ SSC^{lo} monocytes/macrophages from BM to tissues, we reveal different functional fates of monocytes by PDGFR α -lineage origin. F4/80⁺ SSC^{lo} monocytes/macrophages differentiation from upstream hematopoietic progenitors accompanies a dwarfed PDGFR α -lineage compartment in BM. This effect is due to BM-resident macrophages, characterized as Ly6C⁻ Siglec-1⁻ CXCR4⁺, being mostly derived from non-PDGFR α -lineage monocytes. PDGFR α -lineage monocytes specifically occupy the LFA-1^{hi} Itg α _M^{hi} compartment, within which CD115⁺ Ly6C⁺ monocytes dock on the abluminal perivascular surface of BM sinusoids and egress to peripheries. Upon extravasation to some tissues, local recruitment cues favor recruitment of PDGFR α -lineage PB monocytes, which accordingly formulate the tissue macrophage lineage composition (Figure 7).

Compared to LSK progenitors, BM leukocytes, in general, tend to receive reduced contribution from PDGFR α -lineage. In our EdU pulse-trace experiment which labeled newly formed EdU⁺

mice each, two induction batches. (H) Proportion of Pa(lin)⁺ macrophages in healthy (n = 8 mice, 5 batches), LPS-inflamed (n = 3 mice in [A-C]) and atopic dermatitis (n = 5 mice in [E-G]) skin are shown. Proportion of (I) F4/80^{hi} and F4/80⁺ cells, and (J) the respective Ly6C^{+/+} subsets among F4/80⁺ SSC^{lo} monocyte/macrophage in peritoneal cavity (PC) were measured under indicated conditions. (K) PDGFR α -lineage contribution to the indicated subsets was measured under TNF- α stimulation. Reference measurements under steady state are indicated. n = 4 (PB, three induction batches) and five mice (each for inflamed/untreated peritoneal cavity, three induction batches). (L) PDGFR α -lineage contribution in the indicated colonic monocyte/macrophage subsets were measured and compared to the peripheral blood (PB) average measured in Figure 1E (purple dashed line). n = 9 mice, three batches. Error bars, SEM. Individual data are represented by dots. For comparisons of PDGFR α -lineage contribution between tissue compartments or frequencies between cellular subsets in (B-C, F-G, and J-L), one mouse per experiment. Groups were compared by two-tailed t-test in (A-F and I-J), one-way ANOVA followed by Tukey's multiple comparisons in (G and K) and one-sample t-test in (L). *p < 0.05, **p < 0.01, ***p < 0.001, ****p < 0.0001.

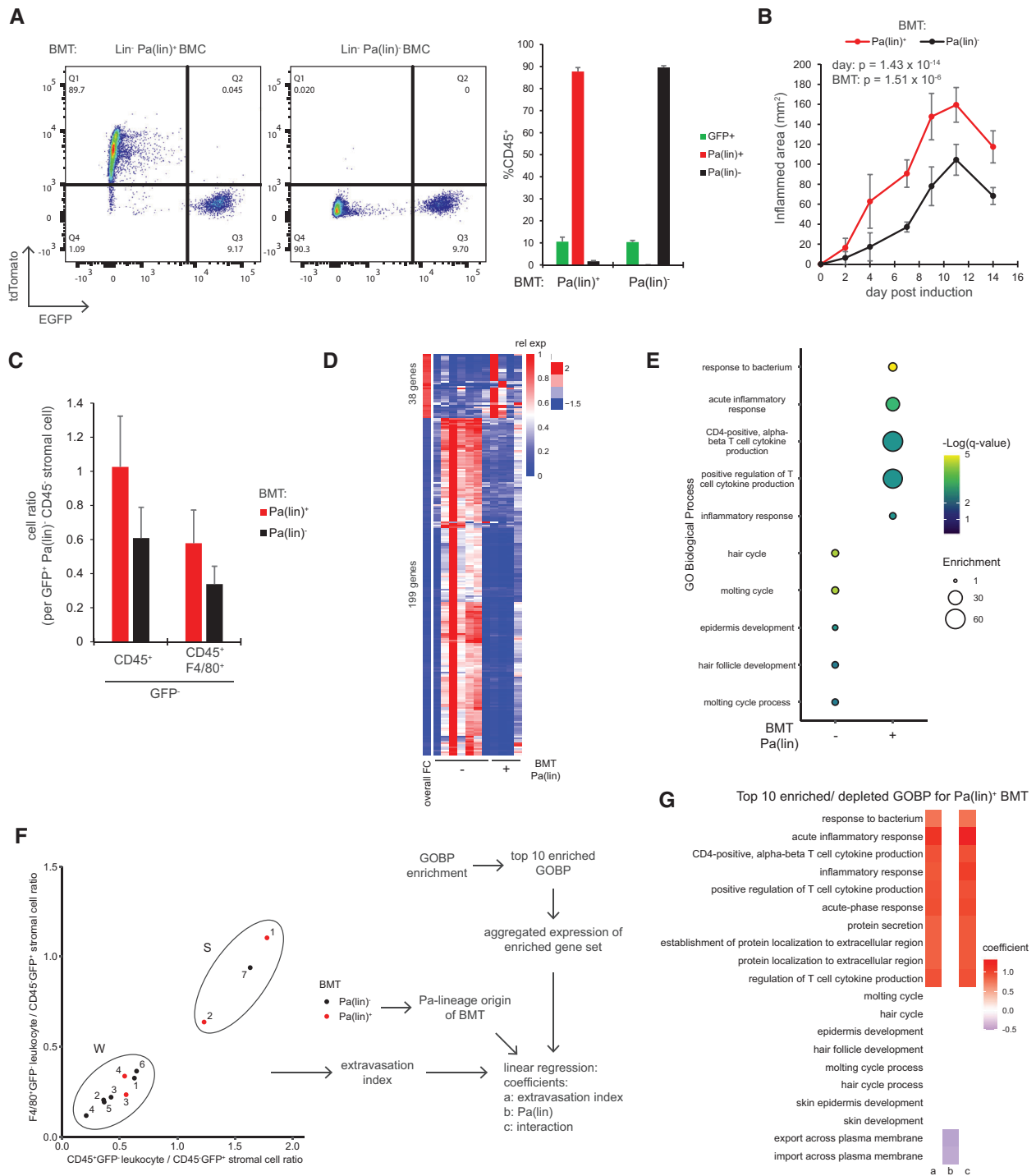


Figure 6. Leukocytes of PDGFR α -lineage origin exert differential influence to the global dermal transcriptome in atopic dermatitis via extravasation. Irradiated EGFP-Tg mice received BM transplantation (BMT) of lin- Pa(lin)⁺ or Pa(lin)⁻ progenitors. After reconstitution for 6 weeks, PB was sampled and analyzed for transplantation efficiency and specificity. (A) Representative flow cytometry plots of mice receiving Pa(lin)⁺ (left) or Pa(lin)⁻ (middle) BMT and quantification (right) are shown. (B) AD was induced by MC903 and inflamed area was monitored during the time course. (C) Leukocytes infiltrated to AD skin were analyzed by flow cytometry on day 14. $n = 4$ Pa(lin)⁺ and 7 Pa(lin)⁻ BMT-chimeric mice in an experiment. Error bars, SEM. Groups were compared by two-way ANOVA in (B) and two-tail t-test in (C). (D) RNA was purified from AD skin of these mice on day 14 postinduction and processed for bulk RNA-sequencing. Top 50% expressing genes showing >twofold change in expression between BMT PDGFR α -lineage origins are shown. (E) Genes in (D) were analyzed for functional enrichment. Top five significant enriched GO biological processes are shown. (F–G) Linear regression was performed with top 10 each of positively or negatively regulated GOBP. (F) Extravasation indices were computed from flow cytometric measurement of leukocyte recruitment in sequenced samples (W: weak, S: strong recruitment group). (G) Aggregated expression of enriched genes in a concerned GOBP was regressed against the extravasation index and PDGFR α -lineage origin of BMT. Estimates of coefficient a , b , and c (associated variable given in [F]) are shown as heatmaps with a p -value cutoff at 0.05.

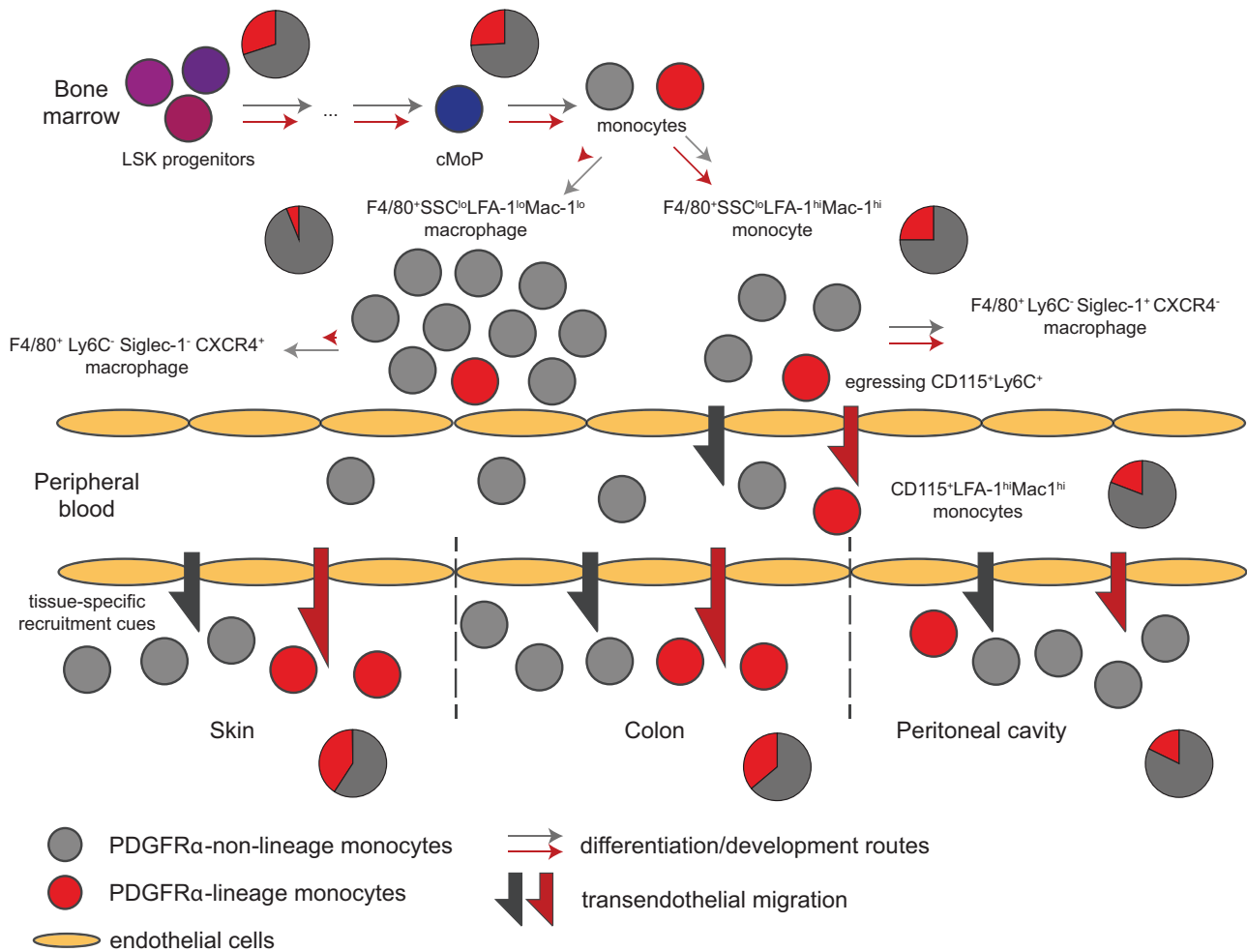


Figure 7. Proposed model showing monocyte fates from biogenesis to trafficking to tissues by PDGFR α -lineage origin. After differentiation from hematopoietic progenitors, monocytes either intravasate to circulation or differentiate to macrophages in BM. BM-resident macrophages are solely derived from non-PDGFR α lineage while both lineages supply trafficking monocytes to circulation as LFA-1^{hi}Mac-1^{hi} CD115⁺Ly6C⁺ cells. Depending on the tissue-specific recruitment cues, PDGFR α -lineage classical monocytes preferentially extravasate to tissues.

BM F4/80⁺SSC^{lo} monocytes/macrophages, PDGFR α -lineage cells seem to be formed slower than non-lineage. It, therefore, implies reluctance of PDGFR α -lineage progenitors to differentiate, likely a gradual process as we detected intermediate PDGFR α -lineage contribution in committed progenitor cMoP and monocytes. Similar reduction in PDGFR α -lineage contribution could be observed in BM B cells. In fetal liver, however, B cells receive similar PDGFR α -lineage contribution as LSK cells [21] suggesting postnatal nature of differentiation bias. Since differentiation decisions are heavily influenced by genomic accessibility which precede transcriptional alteration [35], high-throughput inspection of chromatin structure and accessibility of PDGFR α -lineage/nonlineage LSK might provide insights on their differentiation potentials in vivo. We consider the alternative possibility that PDGFR α -lineage BM leukocytes being short-lived unlikely, since we observed fewer, but not more, PDGFR α -lineage cells in the dead cell gate in our flow cytometric analysis of these BM leukocytes (not shown).

Endothelia are the major barriers controlling the leukocyte traffic across BM, circulation, and tissues. We show in BM that PDGFR α -lineage F4/80⁺SSC^{lo} cells exist mostly as Ly6C⁺ LFA-1^{hi} Itg α_M ^{hi} trafficking monocytes, but not macrophages. Monocytes display a stronger integrin-based adhesive surface which under chemoattraction enables them being better picked up by the endothelium for release into the blood. Unlike PDGFR α -lineage monocytes, non-PDGFR α -lineage monocytes participate in both BM macrophage differentiation and trafficking. Deriving macrophage cultures (Mac^{hi2} and Mac^{lo2}) from trafficking monocytes (LFA-1^{hi} Itg α_M ^{hi}) or BM-resident macrophages (LFA-1^{lo} Itg α_M ^{lo}), our transcriptomic analysis has revealed different functional specialization, TF activities, and gene markers in these macrophages. As Mac^{hi2} is derived from trafficking monocytes, they most likely emerge after extravasation to tissues in vivo. Hence, Mac^{hi2} not only segregates from Mac^{lo2} in location (peripheries vs BM) but the functions as well. Despite the ultimate molecular and functional landscape of macrophages

being the subject of plastic remodeling by vicinity cues [17,36], Mac^{hi2} expresses *Cx3cr1* and CX₃CR1⁺ macrophages have been shown to be derived from circulating monocytes in peripheral tissues of, for example, colon [31] and liver [37]. Another study has shown that FoxM1 activity, strongly detected in Mac^{hi2}, is required for generating CX₃CR1⁺ pathological monocyte-derived osteoclasts in arthritis [38]. On the other hand, Mac^{lo2} differs from the well-known Siglec-1⁺ (which is expressed by Mac^{hi2}) marrow macrophages [39] and represents another subset of marrow-resident macrophages expressing CXCR4. In our single-cell transcriptome dataset that maps BM monocytes/macrophages against PB monocytes (Supporting information Figure S8), while BM-resident monocytes/macrophages express the strongest CXCR4 signal, lower level of CXCR4 expression could be detected in cells mapped to proximity of PB monocytes. This lower expression of CXCR4 seems to be coherent to a previous study [40] describing CXCR4 downregulation during biogenesis of egressing monocytes.

We noticed in some tissues that extravasation of the PDGFR α -lineage fraction had been favored. While the responsible tissue-specific determinants remain unknown, wherever PDGFR α -lineage monocytes are preferentially extravasated, to skin, for instance, the support tends to be more prominent with cMO. An unusual mode of extravasation has been described for peripheral ncMO that they constantly crawl on endothelium in a LFA-1-dependent manner even under steady state to allow quick response to invasion [16]. Likewise, a marginal pool of human CD16⁺ monocytes with high-adhesion molecules expression has been reported [41]. During conversion of cMO to ncMO in PB [10], integrin expression on cell surface is upregulated and become available for activation and EC interaction to support the patrolling behavior observed under steady state [6,7,42]. Distinct from integrin-equivalent PB Pa(lin)^{+/-} cMO, Pa(lin)⁺ ncMO seems to express a lower amount of Itg β 1, which could pose an adhesive disadvantage and counteract potential recruitment advantage. It has been further suggested that ICAM-1 density on the apical endothelial surface, and therefore, should be the leukocyte-EC adhesive strength, influences the subsequent diapedesis route [43]. Hence, the differently regulated ncMO extravasation mechanism might partially account for the selective recruitment of PDGFR α -lineage cMO to tissues. In addition, by mapping single-cell RNA sequencing data of PB monocytes to BM monocytes/macrophages, we could identify subsets of BM monocytes/macrophages that egress to PB. Similar strategies could be pursued in the future to distinguish PB monocytes subsets infiltrating skin/colon and peritoneum, which respectively selected and not selected for PDGFR α -lineage cMO.

Profiling the bulk transcriptome of inflamed skin stroma of BMT-chimeric mice, we found several inflammation-associated functions promoted by the Pa(lin)⁺ hematopoietic transplant. With the prior knowledge of the better extravasation capacity of PDGFR α -lineage monocytes, we attempted to search for affected functions independent of extravasation. Nevertheless, regression analyses using a model separating extravasation and leukocyte lineage origin suggested PDGFR α -lineage leukocytes had

impacted the dermal environment mainly via extravasation. While a portion of extravasated monocytes proceeds to macrophage differentiation, trMF are amongst the leukocytes having extensive crosstalk with tissue stromal cells and have been reported to facilitate tissue remodelling [44–46]. Monocyte-derived macrophages seems to assimilate much of the *bona fide* trMF functionality when placed into the tissue niche [17,47]. Having analyzed with single-cell transcriptomics the macrophage repertoire in inflamed skin, we found macrophages of different PDGFR α -lineage origins displayed skewed functional composition. In particular, PDGFR α -lineage dermal macrophages seem to receive stronger contribution from circulating monocytes as they contain a smaller fraction of *Itgax*⁺*Cd207*⁺*Tgfb1*⁺*Runx3*^{hi} cells (subtype 2) resembling yolk sac-derived Langerhans cells [48–50]. With these insights, we propose extravasated PDGFR α -lineage monocytes differentiate into macrophages with an altered functional profile and further interact with the dermal environment.

Collectively, we document BM monocytes descended from PDGFR α ⁺ embryonic precursors dominantly support macrophage formation in peripheries but not in BM. PDGFR α -lineage BM F4/80⁺SSC^{lo} monocytes mostly occupy the Ly6C⁺ compartment where high integrin expression facilitates adhesion on endothelium and circulation entry. This event routes more PDGFR α -lineage monocytes into peripheries and drives spatial and functional divergence from non-PDGFR α -lineage in macrophages. Our findings imply the diverse embryonic lineage origins of leukocytes might be a determinant in forming the immune functional heterogeneity in adults.

Materials and methods

Animals

Generation of PDGFR α -lineage tracing mice (PDGFR α -CRE;ROSA^{tdTomato}) was previously described [34]. PDGFR α -H2BGFP knock-in reporter mouse line was previously described [22]. EGFP-Tg mice were purchased from Jackson Laboratory (Tg(act-EGFP)Y010sb, #006567) [51]. Unless otherwise specified, 7- to 14-week-old mice of C57BL/6 background (CLEA Japan) were used for experiments. For dermal inflammation, only female mice were used to avoid sporadic inflammation related to fighting/injury. Animals were maintained in a barrier facility under special pathogen-free conditions. All animal experiments were conducted under the guidelines of Osaka University and approved by the Institutional Animal Care and Use Committee of Osaka University Graduate School of Medicine under reference numbers 29-044-067 and 02-075-002.

Cells

Primary dermal ECs (MDMVEC) were isolated and cultured as previously described [52]. To obtain marrow cells (BMC) from femur or tibia, bones were loaded to a pierced 0.6-mL tube on top of a 1.5-mL Eppendorf tube. Centrifugal force of 3000g was

applied for 15 s to obtain cell pellets that were resuspended in PBS containing 2% FBS (resuspension buffer, RB). Vertebra was dissected and crushed in RB. Cells were pelleted and resuspended in RB. To isolate cells from dorsal skin, dissected skin was finely minced with scissors and digested in 0.3% Collagenase A (Roche), 10 U/mL DNase-I (Roche), 0.5 mg/mL dispase-II, 2% FBS in RPMI with agitation at 37°C for 1 h. The digest was passed through a cell strainer of 70-micron pore (Falcon) and resuspended in RB. To isolate cells from colon, fecal contents were first removed from the dissected colon, epithelial cells were then depleted by incubating the colon in HBSS containing 5 mM EDTA with agitation at 37°C for 20 min. The colon was minced and digested in 0.1% Collagenase D (Roche), 30 U/mL DNase-I (Roche), 0.5 mg/mL dispase-II, 2% FBS in RPMI with agitation at 37°C for 1 h. The digest was then passed through a 70-micron pored cell strainer (Falcon) and resuspended in RB.

Dermal inflammation

To induce acute dermal inflammation, 1 µg of LPS or saline ctrl was administered intradermally. After overnight, skin samples were collected for flow cytometric analysis. To induce atopic dermatitis, bidaily/tridaily doses of 5 nmol MC903 in ethanol were applied topically on shaved dorsal skin for six times in 2 weeks. Inflamed ellipse area was monitored by 0.25π (width) \times (length). On day 14, skin samples were collected from inflamed area and prepared for flow cytometric analysis.

Peritoneal inflammation

Mice received a single intraperitoneal dose of 500 ng rm-TNF- α (PeproTech). After overnight, peritoneal lavage was performed by injecting 5 mL PBS containing 1 mM EDTA into PC with gentle rubbing, volume was recovered afterward and prepared for flow cytometric analysis.

BM transplantation

Cells were isolated from femur/tibia of PDGFR α -lineage tracing mice. After bead-removal of lineage⁺ cells, Pa(lin)⁺ and Pa(lin)⁻ cells were sorted by FACS Aria-III (BD Biosciences) and intravenously transplanted to irradiated EGFP-Tg recipients (10 Gy) as previously described [5]. Six weeks were allowed for BM reconstitution before experimentation.

Three-dimensional confocal microscopy

Freshly isolated femurs from PDGFR α -lineage tracing mice were prepared into frozen tissue block as previously described [53] except the fixation was extended to overnight. Sixty-micron thick cryosections were prepared on slides. After rehydration in PBS, the tissue was permeabilized in 0.5% Triton-X-100 in PBS for

15 min and then blocked in 3% BSA and 0.3% Triton-X-100 in PBS (diluent) for 1 h at room temperature. Tissues were stained with 10 µg/mL each of anti-F4/80-Alexa-Fluor-488 (BM8), anti-PECAM-1-Alexa-Fluor-647 (390 and Mec13.3), and anti-Sca1-Brilliant-Violet-421 (D7) (all from Biolegend) in diluent at 4°C in the dark overnight. The slides were then washed and mounted for image stack acquisition by LSM880 (Zeiss). Fiji Image J was used for 3D-stack examination of adherent monocytes on endothelium. Gamma (0.85) was applied to the tdTomato channel for simultaneous visualization of bright perivascular cells and dimmer PDGFR α -lineage leukocytes in BM. For examination of AD skin, samples were process similarly as described except cryosections were prepared in 100 µm-thick and stained with 10 µg/mL each of anti-F4/80-Alexa-Fluor-488 (BM8) and anti-PECAM-1-Alexa-Fluor-647 (Mec13.3) (both from Biolegend).

EdU pulse tracing

One milligram of EdU was injected to mice via intraperitoneal route. EdU-labeled cells were detected by click chemistry with EdU in vivo Kit (Baseclick GmbH) according to manufacturer protocol with modifications. BMC were isolated from femur/tibia and resuspended in 1 mL per limb PBS containing 2% FBS and 200 µL cells were used for each staining/reaction. Standard flow cytometric staining procedures (described in the section “Flow cytometry”) were performed. All subsequent procedures were performed at room temperature in the dark. Cells were fixed with 100 µL 4% PFA for 15 min followed by wash. Permeabilization was performed with 100 µL 0.6 \times permeabilization buffer (Baseclick GmbH) for 20 min. Click reaction concentrate (2 \times) was freshly prepared and 100 µL was directly added to cells followed by quick mixing. The reaction mixture was incubated for 30 min followed by washes with 0.6 \times permeabilization buffer. Samples were resuspended in 0.3 \times permeabilization buffer and analyzed with a flow cytometer (BD FACSCanto II, BD Biosciences).

Competitive adhesion assays

For adhesion on MDMVEC, 96-well plate was coated with 5 µg/mL each of LN411 and LN511 (Biolamina) at 37°C for 1 h. Twenty-thousand WT MDMVEC were seeded per well and cultured to confluence. MDMVEC was stimulated with 0 or 5 nM recombinant murine TNF- α (PeproTech) overnight. BMC obtained from femur, tibia, or vertebra of PDGFR α -lineage tracing mice were resuspended in DMEM buffered with 10 mM HEPES at pH7.0 (assay buffer). Fc receptors were blocked by incubating with 10 µg/mL 2.4G2 at room temperature for 10 min. MDMVEC were washed with assay buffer followed by addition of 2×10^5 BMC labelled with anti-F4/80-APC in 100 µL assay buffer. Cells were allowed to adhere at 37°C for 30 min. Plate was washed for trice to remove nonadherent cells, then the adherent cell complex was dissociated by accutase at 37°C. The proportion of Pa(lin)⁺ F4/80⁺ monocytes in the adherent cells was compared

to input by flow cytometry. For adhesion on CAMs, 96-well plate was coated with 5 $\mu\text{g}/\text{mL}$ of ICAM-1-Fc or VCAM-1-Fc (both from R&D Systems) at 4°C overnight followed by blockade with 1% casein in PBS at room temperature for 1 h. BMC were prepared as described above. The plate was washed and 50 μL of 40 ng/mL CCL_2 was added. Two hundred thousand labelled BMC in 50 μL assay buffer were allowed to adhere on the surface at 37°C for 30 min. Subsequent measurements were performed as described above. In some experiments, 1 or 10 mM MnCl_2 was used instead of CCL_2 as the stimulant.

Flow cytometry

Cells obtained from PDGFR α -lineage tracing mice were analyzed for the proportion of Pa(lin)⁺ (tdTomato⁺) in target cells. Before staining, Fc receptors were blocked with 10 $\mu\text{g}/\text{mL}$ 2.4G2 at room temperature for 10 min. Standard staining procedures were performed on ice to identify target cells using the following antibodies (all from Biolegend): anti-F4/80-APC or -FITC or -BV421 (BM8), anti-MHCII-PE/Cy7 (M5/114.15.2), anti-Ly6C-FITC or -PE (HK1.4), anti-CD19-FITC or -APC (6D5), anti-CD24-PE/Cy7 (M1/69), anti-CD23-PerCP/Cy5.5 (B3B4), anti-IgM-APC (RMM-1), anti-Ly6G-FITC or -APC (1A8), anti-Sca-1-PE/Cy7 (D7), anti-Lineage cocktail-FITC (145-2C11, RB6-8C5, RA3-6B2, Ter-119 and M1/70), anti-Kit-APC (2B8), anti-PECAM-1-PerCP/Cy5.5 (390), anti-LFA-1-PE/Cy7 or -PerCP-Cy5.5 (H155-78), anti-Itgam-BV421 (M1/70), anti-Itga4-PE/Cy7 (R1-2), anti-Itgb1-APC/Cy7 (HMgb1-1), anti-Siglec-1-FITC (3D6.112), anti-CXCR4-PerCP/Cy5.5 (L276F12), anti-CX3CR1-Alexa-Fluor-488 (SA011F11) and anti-CD64-APC (X54-5/7.1). For staining of colonic cells, antibody staining was accompanied by addition of mouse CD45 nanobeads (Biolegend) for magnetic enrichment of leukocytes from colonic digest. Cells, if not fixed, were stained by Sytox-blue to exclude dead cells from analysis. In some experiments, MFI was measured to determine the surface expression level of the antigen. Flow cytometry was performed in compliance to the guidelines described in <https://doi.org/10.1002/eji.201970107>. Gating strategies were described in Supporting information Figures S1–5, 9, and 14.

Transcriptomic library preparation and analyses

For bulk RNA-sequencing, RNA was extracted from cultured macrophages directly by RNeasy Mini Kit (Qiagen) or from AD skin (homogenized under low temperature, liquid N_2) with ISO-GEN (Nippon Gene) and purified by RNeasy Mini Kit (Qiagen). Library was prepared with 12.5 ng of total RNA using a KAPA RNA HyperPrep Kit with RiboErase (HMR) for Illumina (Kapa Biosystems). Briefly, total RNA was depleted for rRNA by hybridization with complementary DNA oligonucleotides, followed by treatment with RNase H and DNase to remove rRNA duplexed with DNA and original DNA oligonucleotides. After fragmenting, the RNA using heat and magnesium, first-

strand cDNA was synthesized using random priming, followed by a combined second strand synthesis and A-tailing process. Libraries were amplified by PCR after the addition of adapters and finally size selected using magnetic beads. The concentration of DNA libraries was determined using the Qubit 3.0 Fluorometer (Thermo Fisher Scientific) and DNA size was analyzed with a 4200 TapeStation (Agilent Technologies). The resulting libraries were sequenced on NextSeq2000 (Illumina) in the paired-end mode (read1: 37bp, index1: 8bp, index2: 8bp, read2: 37bp). Outputs were demultiplexed by bcl2fastq2 (Illumina). After trimming adapter sequences with TrimGalore (<https://github.com/FelixKrueger/TrimGalore>), reads were aligned to the mouse reference genome (mm10, obtained from the iGenomes repository, Illumina). Transcript expression was then quantified using RSEM with STAR. Sequencing counts were normalized by DESeq2 [54] and analyzed with R (version 4.0.3). Transcription activity was analyzed with the DoRotheA algorithm [55,56]. For regression analysis, three parameters were determined for each sample: extravasation index (Extrvs), PDGFR α -lineage (PaLin), and aggregated expression of enriched gene in a concerned enriched GOBP (aggExp). Extrvs is defined as the numeric product of donor-derived CD45⁺ recruitment and donor-derived F4/80⁺ recruitment, both normalized to recipient dermal stromal cells. PaLin is either +1 for Pa(lin)⁺ BMT or –1 for Pa(lin)[–] BMT. To compute aggExp of a gene set, DESeq2-normalized expression was first divided by expression average of all samples for each gene (to balance the expression magnitudes); the computed values from all genes in the gene set were then averaged to give aggExp. Linear regression was performed for each enriched GOBP with the model: $\text{aggExp} = a(\text{Extrvs}) + b(\text{PaLin}) + c(\text{Extrvs} \times \text{PaLin}) + (\text{intercept})$, where a , b , and c are coefficients. Coefficients with $p > 0.1$ were rejected.

For single-cell RNA-sequencing, single cells were prepared from AD skin of PDGFR α -lineage tracing mice. Cells were blocked with 10 $\mu\text{g}/\text{mL}$ 2.4G2 at room temperature for 10 min followed by staining with anti-F4/80-APC (BM8) and biotinylated anti-MHCII (M5/114.15.2) (both from Biolegend). MHCII-expressing cells were positively selected by streptavidin-magnetic beads (Biolegend). Cells were stained by Sytox-blue and viable F4/80⁺ Pa(lin)⁺ and Pa(lin)[–] cells were sorted by FACSARIA-III (BD Biosciences) for single-cell RNA-sequencing. Live cells were sorted into 384-well plates (Eppendorf) using a BD FACSARIA III instrument (Becton Dickinson; 100 μm chip) in single-cell purity mode (1 cell/well). Single-cell RNA-seq libraries construction was previously described [34]. The libraries were sequenced on a NextSeq500 platform (Illumina). Fastq files were aligned to *Mus musculus* GRCm38 reference using STAR aligner (2.7.1a; <https://github.com/alexdobin/STAR>). STARsolo outputs were filtered using the numbers of reads, transcripts, and genes and the percentages of mitochondrial genes and mapped reads for each cell. Data analysis was performed by Monocle3 package [57,58]. Single cells were clustered on Uniform Manifold Approximation and Projection, nonmacrophage clusters were removed and the macrophages were subclustered into subtypes. Subtype proportion of Pa(lin)⁺ and Pa(lin)[–] were computed.

Statistics

Two-tailed Student's *t*-test or Mann–Whitney U-test was used to compare two groups. One-sample *t*-test was used to compare a control-normalized group against an expected value. For multiple comparison, one-way ANOVA or two-way ANOVA was used followed by a posthoc test indicated for each experiment. Data normality was verified by Shapiro–Wilk test. Where applicable, data from multiple sample acquisition batches are shown as pooled summary. An α -value of 0.05 was used to consider statistical significance.

Acknowledgments: This work was partly supported by AMED (Grant number 20ek0109400h0003, to KT) and JSPS KAKENHI (Grant number 19H03682, to KT).

Funding: This work was partly supported by AMED (Grant number 20ek0109400h0003, to KT) and JSPS KAKENHI (Grant number 19H03682, to KT).

Author Contributions: Conceptualization: YTL

Investigation: YTL, SY, ET, TK

Formal analysis: YTL, YO

Writing—original draft: YTL

Writing—review & editing: YTL, KT

Project administration: YTL, KT

Funding acquisition: KT

Conflict of interest: KT is a scientific founder and stockholder of StemRIM. SY, ET, TK, and YO are employees of StemRIM. All other authors declare they have no conflict of interest.

Data availability statement: Sequencing data are available at GEO under accession numbers GSE174721, GSE166854 (bulk RNA-sequencing) and GSE166855 (single-cell RNA-sequencing). The data that support the findings of this study are available in the article and the supplementary material of this article. All other data described in this study are available on reasonable request to correspondence.

Peer review: The peer review history for this article is available at <https://publons.com/publon/10.1002/eji.202149479>

REFERENCES

- Nourshargh, S., Alon, R. Leukocyte migration into inflamed tissues. *Immunity*. 2014. 41 694–707.
- Zarbock, A., Ley, K., Mcever, R P., Hidalgo, A. Leukocyte ligands for endothelial selectins: specialized glycoconjugates that mediate rolling and signaling under flow. *Blood*. 2011. 118 6743–6751.
- Kunkel, E J., Ley, K. Distinct phenotype of E-selectin-deficient mice. E-selectin is required for slow leukocyte rolling in vivo. *Circ. Res.* 1996. 79 1196–1204.
- Yago, T., Shao, B., Miner, J J., Yao, L., Klopocki, A G., Maeda, K., Coggeshall, K. M., et al., E-selectin engages PSGL-1 and CD44 through a common signaling pathway to induce integrin alphaLbeta2-mediated slow leukocyte rolling. *Blood*. 2010. 116 485–494.
- Li, Yu-T, Goswami, D., Follmer, M., Artz, A., Pacheco-Blanco, M., Vestweber, D. Blood flow guides sequential support of neutrophil arrest and diapedesis by PILR- β 1 and PILR- α . *eLife*. 2019. 8 e47642.
- Ley, K., Laudanna, C., Cybulsky, M I., Nourshargh, S. Getting to the site of inflammation: the leukocyte adhesion cascade updated. *Nat. Rev. Immunol.* 2007. 7 678–689.
- Vestweber, D. How leukocytes cross the vascular endothelium. *Nat. Rev. Immunol.* 2015. 15 692–704.
- Fogg, D K., Sibon, C., Miled, C., Jung, S., Aucouturier, P., Littman, D R., Cumano, A., et al., A clonogenic bone marrow progenitor specific for macrophages and dendritic cells. *Science*. 2006. 311 83–87.
- Hettinger, J., Richards, D. M., Hansson, J., Barra, M. M., Joschko, A. - C., Krijgsveld, J., Feuerer, M. Origin of monocytes and macrophages in a committed progenitor. *Nat. Immunol.* 2013. 14 821–830.
- Yona, S., Kim, Ki-W, Wolf, Y., Mildner, A., Varol, D., Breker, M., Strauss-Ayali, D., et al., Fate mapping reveals origins and dynamics of monocytes and tissue macrophages under homeostasis. *Immunity*. 2013. 38 79–91.
- Lewis, N D., Haxhinasto, S A., Anderson, S M., Stefanopoulos, D E., Fogal, S E., Adusumalli, P., Desai, S N., et al., Circulating monocytes are reduced by sphingosine-1-phosphate receptor modulators independently of S1P3. *J. Immunol.* 2013. 190 3533–3540.
- Kratofil, R M., Kubes, P., Deniset, J F. Monocyte conversion during inflammation and injury. *Arterioscler. Thromb. Vasc. Biol.* 2017. 37 35–42.
- Serbina, N. V., Pamer, E. G. Monocyte emigration from bone marrow during bacterial infection requires signals mediated by chemokine receptor CCR2. *Nat. Immunol.* 2006. 7 311–317.
- Sarin, H. Physiologic upper limits of pore size of different blood capillary types and another perspective on the dual pore theory of microvascular permeability. *J. Angiogenesis Res.* 2010. 2: 14.
- Inoue, S., Osmond, D. G. Basement membrane of mouse bone marrow sinusoids shows distinctive structure and proteoglycan composition: a high resolution ultrastructural study. *Anat. Rec.* 2001. 264 294–304.
- Auffray, C., Fogg, D., Garfa, M., Elain, G., Join-Lambert, O., Kayal, S., Sarnacki, S., et al., Monitoring of blood vessels and tissues by a population of monocytes with patrolling behavior. *Science*. 2007. 317 666–670.
- Lavin, Y., Winter, D., Blecher-Gonen, R., David, E., Keren-Shaul, H., Merad, M., Jung, S., et al., Tissue-resident macrophage enhancer landscapes are shaped by the local microenvironment. *Cell*. 2014. 159 1312–1326.
- Kourtzelis, I., Li, X., Mitroulis, I., Gresser, D., Kajikawa, T., Wang, B., Grzybek, M., et al., DEL-1 promotes macrophage efferocytosis and clearance of inflammation. *Nat. Immunol.* 2019. 20 40–49.
- Hashimoto, D., Chow, A., Noizat, C., Teo, P., Beasley, M. B., Leboeuf, M., Becker, C. D., et al., Tissue-resident macrophages self-maintain locally throughout adult life with minimal contribution from circulating monocytes. *Immunity*. 2013. 38 792–804.
- Lugus, J J., Park, C., Ma, Y D., Choi, K. Both primitive and definitive blood cells are derived from Flk-1+ mesoderm. *Blood*. 2009. 113 563–566.
- Ding, G., Tanaka, Y., Hayashi, M., Nishikawa, S. - I., Kataoka, H. PDGF receptor alpha+ mesoderm contributes to endothelial and hematopoietic cells in mice. *Dev. Dyn. Off. Publ. Am. Assoc. Anat.* 2013. 242 254–268.

- 22 Tamai, K., Yamazaki, T., Chino, T., Ishii, M., Otsuru, S., Kikuchi, Y., Iinuma, S., et al., PDGFR α -positive cells in bone marrow are mobilized by high mobility group box 1 (HMGB1) to regenerate injured epithelia. *Proc. Natl. Acad. Sci. U. S. A.* 2011. **108** 6609–6614.
- 23 Evrard, M., Kwok, I W.H., Chong, S. Z., Teng, K W.W., Becht, E., Chen, J., Sieow, J. L., et al., Developmental analysis of bone marrow neutrophils reveals populations specialized in expansion, trafficking, and effector functions. *Immunity*. 2018. **48** 364–379.e8.
- 24 Itkin, T., Gur-Cohen, S., Spencer, J A., Schajnovitz, A., Ramasamy, S K., Kusumbe, A P., Ledergor, G., et al., Distinct bone marrow blood vessels differentially regulate haematopoiesis. *Nature*. 2016. **532** 323–328.
- 25 Takagi, J., Petre, B M., Walz, T., Springer, T A. Global conformational rearrangements in integrin extracellular domains in outside-in and inside-out signaling. *Cell*. 2002. **110** 599–611.
- 26 Sen, M., Koksai, A C., Yuki, K., Wang, J., Springer, T A. Ligand- and cation-induced structural alterations of the leukocyte integrin LFA-1. *J. Biol. Chem.* 2018. **293** 6565–6577.
- 27 Issekutz, T. B. In vivo blood monocyte migration to acute inflammatory reactions, IL-1 α , TNF- α , IFN- γ , and C5a utilizes LFA-1, Mac-1, and VLA-4. The relative importance of each integrin. *J. Immunol. Baltimore (Md)* 1950. **154** 6533–6540.
- 28 Naidoo, K., Jagot, F., Van Den Elsen, L., Pellefigues, C., Jones, A., Luo, H., Johnston, K., et al., Eosinophils determine dermal thickening and water loss in an MC903 model of atopic dermatitis. *J. Invest. Dermatol.* 2018. **138** 2606–2616.
- 29 Tamoutounour, S., Williams, M., Montanana Sanchis, F., Liu, H., Therorst, D., Malosse, C., Pollet, E., et al., Origins and functional specialization of macrophages and of conventional and monocyte-derived dendritic cells in mouse skin. *Immunity*. 2013. **39** 925–938.
- 30 Ghosn, E. E. B., Cassado, A. A., Govoni, G. R., Fukuhara, T., Yang, Y., Monack, D. M., Bortoluci, K. R., et al., Two physically, functionally, and developmentally distinct peritoneal macrophage subsets. *Proc. Natl. Acad. Sci. U. S. A.* 2010. **107** 2568–2573.
- 31 Bogunovic, M., Ginhoux, F., Helft, J., Shang, L., Hashimoto, D., Greter, M., Liu, K., et al., Origin of the lamina propria dendritic cell network. *Immunity*. 2009. **31** 513–525.
- 32 Korotkevich, G., Sukhov, V., Sergushichev, A. Fast gene set enrichment analysis. bioRxiv. Published online October 22, 2019:060012.
- 33 Ganuza, M., Hall, T., Finkelstein, D., Chabot, A., Kang, G., Mckinney-Freeman, S. Lifelong haematopoiesis is established by hundreds of precursors throughout mammalian ontogeny. *Nat. Cell Biol.* 2017. **19** 1153–1163.
- 34 Miura, A., Shimbo, T., Kitayama, T., Ouchi, Y., Yamazaki, S., Nishida, M., Takaki, E., et al., Contribution of PDGFR α lineage cells in adult mouse hematopoiesis. *Biochem. Biophys. Res. Commun.* 2020. **534** 186–192.
- 35 Ma, S., Zhang, B., Lafave, L M., Earl, A S., Chiang, Z., Hu, Y., Ding, J., et al., Chromatin potential identified by shared single-cell profiling of RNA and chromatin. *Cell*. 2020. **183** 1103–1116.
- 36 Gautier, E. L., Shay, T., Miller, J., Greter, M., Jakubzick, C., Ivanov, S., Helft, J., et al., Gene-expression profiles and transcriptional regulatory pathways that underlie the identity and diversity of mouse tissue macrophages. *Nat. Immunol.* 2012. **13** 1118–1128.
- 37 Viebahn, C S., Benseker, V., Holz, L E., Elsegood, C L., Vo, M., Bertolino, P., Ganss, R., et al., Invading macrophages play a major role in the liver progenitor cell response to chronic liver injury. *J. Hepatol.* 2010. **53** 500–507.
- 38 Hasegawa, T., Kikuta, J., Sudo, T., Matsuura, Y., Matsui, T., Simmons, S., Ebina, K., et al., Identification of a novel arthritis-associated osteoclast precursor macrophage regulated by FoxM1. *Nat. Immunol.* 2019. **20** 1631–1643.
- 39 Chow, A., Lucas, D., Hidalgo, A., Méndez-Ferrer, S., Hashimoto, D., Scheiermann, C., Battista, M., et al., Bone marrow CD169+ macrophages promote the retention of hematopoietic stem and progenitor cells in the mesenchymal stem cell niche. *J. Exp. Med.* 2011. **208** 261–271.
- 40 Chong, S. Z., Evrard, M., Devi, S., Chen, J., Lim, J. Y., See, P., Zhang, Y., et al., CXCR4 identifies transitional bone marrow premonocytes that replenish the mature monocyte pool for peripheral responses. *J. Exp. Med.* 2016. **213** 2293–2314.
- 41 Steppich, B., Dayyani, F., Gruber, R., Lorenz, R., Mack, M., Ziegler-Heitbrock, H. W. L. Selective mobilization of CD14(+)CD16(+) monocytes by exercise. *Am. J. Physiol. Cell Physiol.* 2000. **279** C578–C586.
- 42 Mcever, R P. Selectins: initiators of leucocyte adhesion and signalling at the vascular wall. *Cardiovasc. Res.* 2015. **107** 331–339.
- 43 Abadier, M., Haghayegh Jahromi, N., Cardoso Alves, L., Boscacci, R., Vestweber, D., Barnum, S., Deutsch, U., et al., Cell surface levels of endothelial ICAM-1 influence the transcellular or paracellular T-cell diapedesis across the blood-brain barrier. *Eur. J. Immunol.* 2015. **45** 1043–1058.
- 44 Okabe, Y., Medzhitov, R. Tissue-specific signals control reversible program of localization and functional polarization of macrophages. *Cell*. 2014. **157** 832–844.
- 45 Nguyen, K D., Qiu, Y., Cui, X., Goh, Y. P. S., Mwangi, J., David, T., Mukundan, L., et al., Alternatively activated macrophages produce catecholamines to sustain adaptive thermogenesis. *Nature*. 2011. **480** 104–108.
- 46 Paolicelli, R C., Bolasco, G., Pagani, F., Maggi, L., Scianni, M., Panzanelli, P., Giustetto, M., et al., Synaptic pruning by microglia is necessary for normal brain development. *Science*. 2011. **333** 1456–1458.
- 47 Suzuki, T., Arumugam, P., Sakagami, T., Lachmann, N., Chalk, C., Sallese, A., Abe, S., et al., Pulmonary macrophage transplantation therapy. *Nature*. 2014. **514** 450–454.
- 48 Gomez Peidiguero, E., Klapproth, K., Schulz, C., Busch, K., Azzoni, E., Crozet, L., Garner, H., et al., Tissue-resident macrophages originate from yolk-sac-derived erythro-myeloid progenitors. *Nature*. 2015. **518** 547–551.
- 49 Borkowski, T A., Letterio, J J., Farr, A G., Udey, M C. A role for endogenous transforming growth factor beta 1 in Langerhans cell biology: the skin of transforming growth factor beta 1 null mice is devoid of epidermal Langerhans cells. *J. Exp. Med.* 1996. **184** 2417–2422.
- 50 Chopin, M., Seillet, C., Chevrier, S., Wu, Li, Wang, H., Morse, H C., Belz, G T., et al., Langerhans cells are generated by two distinct PU.1-dependent transcriptional networks. *J. Exp. Med.* 2013. **210** 2967–2980.
- 51 Okabe, M., Ikawa, M., Kominami, K., Nakanishi, T., Nishimune, Y. “Green mice” as a source of ubiquitous green cells. *FEBS Lett.* 1997. **407** 313–319.
- 52 Frye, M., Dierkes, M., Küppers, V., Vockel, M., Tomm, J., Zeuschner, D., Rossaint, J., et al., Interfering with VE-PTP stabilizes endothelial junctions in vivo via Tie-2 in the absence of VE-cadherin. *J. Exp. Med.* 2015. **212** 2267–2287.
- 53 Kusumbe, A P., Ramasamy, S K., Adams, R H. Coupling of angiogenesis and osteogenesis by a specific vessel subtype in bone. *Nature*. 2014. **507** 323–328.
- 54 Love, M. I., Huber, W., Anders, S. Moderated estimation of fold change and dispersion for RNA-seq data with DESeq2. *Genome Biol.* 2014. **15** 550.
- 55 Alvarez, M. J., Shen, Y., Giorgi, F. M., Lachmann, A., Ding, B. B., Ye, B. H., Califano, A. Functional characterization of somatic mutations in cancer using network-based inference of protein activity. *Nat. Genet.* 2016. **48** 838–847.
- 56 Holland, C H., Szalai, B., Saez-Rodríguez, J. Transfer of regulatory knowledge from human to mouse for functional genomics analysis. *Biochim. Biophys. Acta BBA—Gene Regul. Mech.* 2020. **1863** 194431.
- 57 Trapnell, C., Cacchiarelli, D., Grimsby, J., Pokharel, P., Li, S., Morse, M., Lennon, N. J., et al., The dynamics and regulators of cell fate decisions

are revealed by pseudotemporal ordering of single cells. *Nat. Biotechnol.* 2014. **32** 381–386.

58 Cao, J., Spielmann, M., Qiu, X., Huang, X., Ibrahim, D M., Hill, A J., Zhang, F., et al., The single-cell transcriptional landscape of mammalian organogenesis. *Nature*. 2019. **566** 496–502.

Abbreviations: **AD:** atopic dermatitis · **BMC:** Bone marrow cells · **BMT:** BM transplantation · **CAMs:** cell adhesion molecules · **cMoP:** common monocyte progenitor · **EC:** endothelial cell · **GO:** Gene ontology · **GOBP:** GO biological processes · **HSPC:** hematopoietic stem and progenitor cells · **LSK:** Lineage- Sca1+ Kit+ · **MDP:** macrophage and DC progenitor · **PB:** peripheral blood · **PC:** peritoneal cavity · **trMF:** tissue-resident macrophages · **TF:** transcription factor

Full correspondence: Dr. Yu-Tung Li and Dr. Katsuto Tamai, Department of Stem Cell Therapy Science, Graduate School of Medicine, Osaka University, Suita 565–0871, Japan
e-mails: tomli_yt@sts.med.osaka-u.ac.jp;
tamai@gts.med.osaka-u.ac.jp

Received: 1/7/2021

Revised: 11/10/2021

Accepted: 25/10/2021

Accepted article online: 28/10/2021